Geoscience Frontiers 6 (2015) 481–501

HOSTED BY

Contents lists available at ScienceDirect

China University of Geosciences (Beijing)

Geoscience Frontiers

journal homepage: www.elsevier.com/locate/gsf

Research paper

A new method of discriminating different types of post-Archean ophiolitic basalts and their tectonic significance using Th-Nb and Ce-Dy-Yb systematics

Emilio Saccani*

Dipartimento di Fisica e Scienze della Terra, Università di Ferrara, Via Saragat 1, 44122 Ferrara, Italy

ARTICLE INFO

Article history:
Received 22 December 2013
Received in revised form
7 March 2014
Accepted 11 March 2014
Available online 25 March 2014

Keywords:
Basalts
Ophiolite
Discrimination diagram
Trace elements
Plate tectonics

ABSTRACT

In this paper, a new discrimination diagram using absolute measures of Th and Nb is applied to post-Archean ophiolites to best discriminate a large number of different ophiolitic basalts. This diagram was obtained using >2000 known ophiolitic basalts and was tested using ~560 modern rocks from known tectonic settings. Ten different basaltic varieties from worldwide ophiolitic complexes have been examined. They include two basaltic types that have never been considered before, which are: (1) medium-Ti basalts (MTB) generated at nascent forearc settings; (2) a type of mid-ocean ridge basalts showing garnet signature (G-MORB) that characterizes Alpine-type (i.e., non volcanic) rifted margins and ocean-continent transition zones (OCTZ). In the Th-Nb diagram, basalts generated in oceanic subduction-unrelated settings, rifted margins, and OCTZ can be distinguished from subduction-related basalts with a misclassification rate <1%. This diagram highlights the chemical variation of oceanic, rifted margin, and OCTZ basalts from depleted compositions to progressively more enriched compositions reflecting, in turn, the variance of source composition and degree of melting within the MORB-OIB array. It also highlights the chemical contributions of enriched (OIB-type) components to mantle sources. Enrichment of Th relative to Nb is particularly effective for highlighting crustal input via subduction or crustal contamination. Basalts formed at continental margin arcs and island arc with a complex polygenetic crust can be distinguished from those generated in intra-oceanic arcs in supra-subduction zones (SSZ) with a misclassification rate <1%. Within the SSZ group, two sub-settings can be recognized with a misclassification rate <0.5%. They are: (1) SSZ influenced by chemical contribution from subduction-derived components (forearc and intra-arc sub-settings) characterized by island arc tholeiitic (IAT) and boninitic basalts; (2) SSZ with no contribution from subduction-derived components (nascent forearc sub-settings) characterized by MTBs and depleted-MORBs. Two additional discrimination diagrams are proposed: (1) a Dy-Yb diagram is used for discriminating boninite and IAT basalts; (2) a Ce/Yb-Dy/Yb diagram is used for discriminating G-MORBs and normal MORBs. The proposed method may effectively assist in recovering the tectonic affinity of ancient ophiolites, which is fundamental for establishing the geodynamic evolution of ancient oceanic and continental domains, as well as orogenic belts.

1. Introduction

Ophiolites are relicts of oceanic lithosphere, which commonly delineate suture zones between continental terranes and provide fundamental constraints on the geodynamic evolution of ancient oceanic basins and surrounding continental areas. In fact, ophiolites are interpreted to form in a wide variety of plate tectonic settings including oceanic spreading ridges, hot spots, and supra-subduction zone (SSZ) environments, such as intra-oceanic arcs, continental arcs, forearcs, and back-arcs (e.g., Dilek and Furnes, 2011). Therefore, different rocks or rock associations found in ophiolitic complexes preserve records of tectono-magmatic events that occurred during distinct phases of oceanic development, from continental rifting to oceanic spreading, subduction, accretion and continental collision (see the "life cycle of ophiolites" in Shervais, 2001). Recognition of the tectonic affinity of ancient ophiolites is therefore a fundamental problem for all scientists working on this topic.

* Tel.: +39 (0) 532 974719; fax: +39 (0) 532 974767.
E-mail address: sac@unife.it.
Peer-review under responsibility of China University of Geosciences (Beijing)

1674-9871/$ – see front matter © 2015, China University of Geosciences (Beijing) and Peking University. Production and hosting by Elsevier B.V. All rights reserved.
http://dx.doi.org/10.1016/j.gsf.2014.03.006

In addition to field data, basalt geochemistry is commonly used for recognizing a variety of different tectonic settings, as well as the nature of mantle sources. Tectonic discrimination diagrams based on both major and trace elements have been a common technique for addressing this problem since the early 1970s (e.g., Pearce and Cann, 1973; Pearce and Norry, 1979; Wood, 1980; Pearce, 1982; Shervais, 1982; Beccaluva et al., 1983; Meschede, 1986; Cabanis and Lécolle, 1989; Vermeesch, 2006; Agrawal et al., 2008; Pearce, 2008). However, according to many authors (e.g., Wang and Glover, 1992; Vermeesch, 2006; Agrawal et al., 2008), the most common tectonic discrimination diagrams are not fully satisfactory, particularly if used in isolation. Auspiciously, when using a combination of two, three, or more diagrams, results are generally satisfactory.

The fact that current tectonic discrimination diagrams are not fully satisfactory may be related to several potential issues: (1) some popular discrimination diagrams (e.g., Pearce and Cann, 1973) are based on the arithmetic means of multiple samples, which has no physical meaning (Vermeesch, 2006); (2) samples used in creating these diagrams were perhaps not statistically representative (either limited number of samples or limited number of places), as for example in Wood (1980); (3) in some diagrams (e.g., Wood, 1980), some of the data were not original, as they were calculated using concentrations of other elements; (4) commonly, each diagram includes only a limited number of the various basaltic types that can be found in ophiolites; (5) the propagation of analytical errors when using element ratios or triangular diagrams is hard to evaluate; (6) implications of the constant-sum constraint of geochemical data, which are particularly important in triangular diagrams, were overlooked; (7) implications of the spurious correlations (Chayes, 1949) associated with the use of element ratios were ignored.

Some attempts at improving the reliability of tectonic discrimination diagrams have however been made. Agrawal (1999) and Agrawal et al. (2008) suggested the use of the statistical technique of linear discriminant analysis for defining class boundaries objectively. Verma et al. (2006) and Vermeesch (2006) solved the problem of statistical treatment for constant-sum data by using log-transformed ratios of elements, significantly increasing the success rate in identifying four types of basaltic rocks. However, in spite of the important advances introduced by these statistical techniques, the methods proposed by these authors are rarely used in literature.

It is not the intention of this paper to re-examine previously proposed discrimination diagrams. Rather, in order to provide ready-to-use diagrams that can discriminate the largest possible number of tectonic settings of formation of ophiolitic basalts, the present paper proposes a set of new, very simple discrimination diagrams based on the relatively immobile high-field-strength element (HFSE) Nb, Th, Ce, Dy, and Yb. Ten different varieties of basaltic rocks from worldwide ophiolitic complexes (Fig. 1) are taken into account in these diagrams, including two basaltic varieties that have never been considered in any discrimination diagram so far presented in literature. They are: (1) basalts showing a marked garnet signature that are generated at Alpine Tethys-type (Iberian-type) ocean-continent transition zones (OCTZ) (e.g., Montanini et al., 2008; Saccani et al., 2008a) and (2) basalts with geochemical features that are intermediate between those of normal-type mid-ocean ridge basalts (N-MORB) and those of island arc tholeiites (IAT), which are generated at nascent intra-oceanic arcs (e.g., Bortolotti et al., 1996, 2002; Bébien et al., 2000; Hoeck et al., 2002).

Although recent ophiolite classification schemes have been applied to the search for Archean oceanic basalts (e.g., Pearce, 2008; Dilek and Furnes, 2011), this argument will not be discussed in this paper. The Archean mantle was very different from the post-Archean one and many of its characteristics (i.e., composition, melting degree and melting depth, mineral phases present on the liquidus during the melting) are in direct contrast to what observed from Proterozoic onward (e.g., Griffin et al., 2003; Francis, 2003). Therefore, the application of the discrimination diagrams proposed in this paper to Archean rocks will require an exhaustive discussion of the petrogenetic conditions acting during Archean times, which is beyond the scope of this paper.

2. Basalt types, classification of ophiolites, and tectonic setting

In this section, an overview of the different varieties of basaltic rocks used in this paper, their tectonic setting of formation, and their occurrence in different ophiolitic-types will be presented. The classification of ophiolites and related tectonic settings of formation used herein is largely based on the classification recently proposed by Dilek and Furnes (2011). Commonly known basaltic types (e.g., mid-ocean ridge basalts, boninites, alkaline basalts, etc.) will be illustrated briefly, whereas two basaltic types that have never so far been considered in any discrimination diagram will be described more thoroughly.

2.1. Oceanic ridge and intra-plate basalts

Mid-ocean ridge basalts may form in a variety of tectonic settings including mid-ocean ridges and backarc spreading ridges (Dilek and Furnes, 2011). MORBs basically include three distinct chemical varieties: normal-type, enriched-type (E-), and plume-type (P-). According to Pearce (2008), N-MORB and E-MORB have compositions that are more depleted and more enriched, respectively, than primitive mantle-derived magmas. Commonly, N-MORBs form at plume-distal mid-ocean ridges, trench-proximal mid-ocean ridges, or trench-distal backarc spreading ridges (Dilek and Furnes, 2011) but also at non-volcanic and transitional-type rifted margins (see Robertson, 2007 for the definition of rifted margins). In these settings, they can be associated with E-MORBs. P-MORBs may form at, or close to plume-proximal spreading ridges, as well as at oceanic plateaus (e.g., Caribbean Plateau; Kerr et al., 1998), where they are often associated with E-MORBs and/or alkaline ocean island basalts (OIB). Commonly, P-MORBs have a chemistry that is indicative of variable garnet influence (Pearce, 2008). Although a sharp distinction between E-MORBs and P-MORBs cannot be made on a chemical basis, the latter commonly have comparatively more enriched trace element patterns with respect to the former (Pearce, 2008). Relatively more enriched P-MORBs have incompatible trace element and REE (rare earth element) patterns that overlap those of OIBs. Nonetheless, the former commonly show a sub-alkaline or transitional nature (e.g., $Nb/Y < 1$; Pearce, 1982), whereas the latter have a clear alkaline nature (e.g., $Nb/Y > 1$).

A particular type of N-MORB is represented by basalts, which typically crop out in several Alpine-type Tethyan ophiolites, that is: in the western Alps, northern Apennine, Alpine Corsica, and Calabria. As shown in Fig. 2, these basalts can be distinguished from typical N-MORBs as they are characterized by significant depletion in heavy REE (HREE) with respect to medium REE (MREE). In fact, the $(Sm/Yb)_N$ ratios are higher than that of typical N-MORB ($Sm_N/Yb_N = 0.96$, Sun and McDonough, 1989), as they range from 1.25 to 1.81 (Montanini et al., 2008; Saccani et al., 2008a). Such a HREE/MREE depletion is interpreted as a clear garnet signature of their mantle sources. Montanini et al. (2008) and Saccani et al. (2008a) suggested that these basalts were originated from partial melting of a depleted mantle source characterized by garnet-bearing mafic

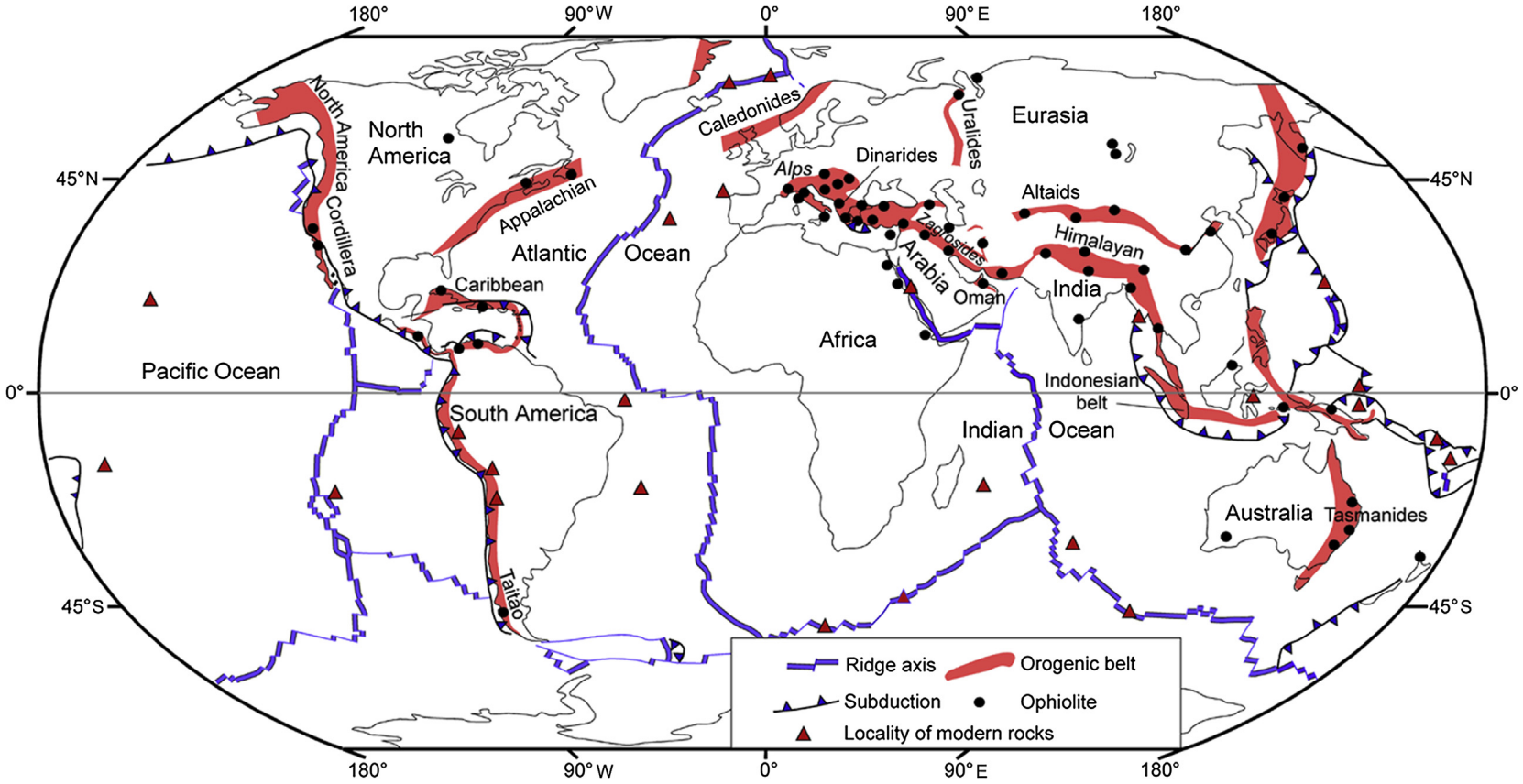

Figure 1. Global distribution of major Proterozoic and Phanerozoic ophiolitic belts, as well as location of ophiolites and modern rocks used in this paper (for details, see Table 1).

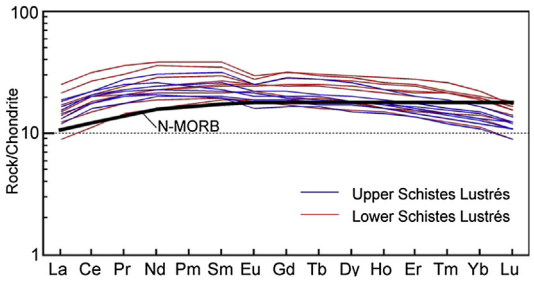

Figure 2. Chondrite-normalized REE patterns for garnet-influenced MORBs from the Jurassic upper and lower schistes Lustrés of the Alpine Corsica ophiolites (data from Saccani et al., 2008a). Normalizing values are from Sun and McDonough (1989).

layers. They usually occur in association with N-MORBs and E-MORBs, which are commonly considered as the products of low degrees of melting of less-depleted subcontinental lithospheric mantle and upwelling asthenosphere (Rampone et al., 2005). These basalts are exclusively found in the Continental Margin (CM) ophiolites of Dilek and Furnes (2011). CM ophiolites commonly represent fragments of the ocean-continent transition zone forming during the continental breakup and the following early stages of oceanic basin evolution. Similar modern OCTZ include the Iberia and Red Sea–western Arabia rifted margins (Dilek and Furnes, 2011). Since these basalts, in contrast with other varieties of MORBs, are exclusively indicative of CM ophiolites, they will be treated as a separate type of ophiolitic basalts that will hereafter named G-MORB (garnet-influenced MORB). Although these basalts form in CM ophiolites, G-MORB is used in this paper instead of C-MORB (continental margin MORB of Dilek and Furnes, 2011) because several authors (e.g., Pearce, 2008) have proposed the term C-MORB for describing crustally contaminated (C) ophiolites, as for example the Taitao ophiolite in Chile, which formed at the trench-proximal Chile Rise (Karsten et al., 1996).

Alkaline basalts (AB) found in ophiolites mainly include rocks formed at seamounts (OIB). They mainly occur as tectonic slices or

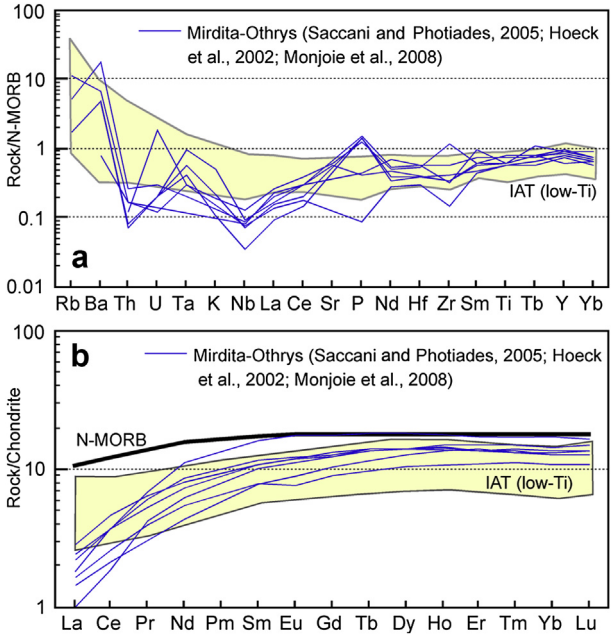

Figure 3. N-MORB normalized incompatible element (a) and chondrite-normalized REE (b) patterns for Jurassic medium-Ti basalts (MTB) from the Albanide-Hellenide ophiolites. Normalizing values are from Sun and McDonough (1989).

blocks incorporated into mélanges, that is as accreted fragments of oceanic terranes. However, ABs formed at volcanic-type and transitional-type rifted margins (Robertson, 2007) are locally found in some ophiolitic complexes, as in the Oman marginal sequences (e.g., Lapierre et al., 2004) and in the Carboniferous Misho mafic complex in Iran (Saccani et al., 2013a). Many AB, as well as P-MORB sequences, do not strictly match the "ophiolite" definition of the Penrose Conference (Anonymous, 1972). In fact, some authors (e.g., Hauff et al., 1997) prefer to term these sequences as "oceanic igneous terranes" rather than "ophiolites". Nonetheless, some AB and P-MORB sequences have plutonic rocks and lavas (e.g., Nicoya complex in Costa Rica, Beccaluva et al., 1999) or plutonic rocks, sheeted dykes and lavas (e.g., Misho complex in Iran, Saccani et al., 2013a) that could fit the "incomplete ophiolite" definition of the Penrose Conference Participants (1972). Alkaline basalts show a clear plume-type chemical signature and variable garnet influence, which result in marked LILE (large ion lithophile element) enrichment and high LREE/HREE ratios (LREE: light REE).

2.2. Subduction-related and backarc basin basalts

SSZ ophiolites form in the extending upper plates of subduction zones, as in the modern Izu-Bonin-Mariana and Tonga-Kermadec arc-trench rollback systems (Dilek and Furnes, 2011 and references therein). Due to the complexity of SSZ settings, several different basaltic varieties may form in these environments.

Boninitic and island arc tholeiitic basalts, corresponding to the very low-Ti and low-Ti basalts of Beccaluva et al. (1983), respectively, typically form in intra-oceanic island arc settings. IAT basalts have HFSE and REE depletion consistent with a genesis from partial melting of depleted mantle sources that experienced previous melt extraction. Very low-Ti (boninitic) basalts show more pronounced REE and HFSE overall depletion when compared to IATs. These features are commonly attributed to high degrees of partial melting of refractory mantle sources that underwent multi-stage melt extraction.

Both IATs and boninites show variable enrichments in LILE and LREE compared to HFSE and REE, respectively suggesting that the depleted mantle sources underwent metasomatic enrichment from subduction-derived fluids in the supra-subduction mantle wedge (e.g., Pearce, 1982; Beccaluva and Serri, 1988; Dilek and Thy, 2009).

A particular, though rare, type of SSZ basalts that deserves to be treated as a specific variety is represented by basalts showing geochemical features that are generally intermediate between those of high-Ti (i.e., N-MORB) and those of low-Ti basalts. For this reason, they will be hereafter-named medium-Ti basalts (MTB). These rocks have been recognized in the Dinaride-Hellenide ophiolites by several authors. They have previously been described as MORB/IAT intermediate basalts (Bortolotti et al., 1996, 2002; Photiades et al., 2003; Saccani and Photiades, 2005), Low Zr–high Cr basalts (Bébien et al., 2000), and intermediate-Ti basalts (Hoeck et al., 2002). They occur mostly as pillow basalts in both coherent ophiolitic volcanic sequences and in ophiolitic mélange. When occurring in coherent ophiolitic volcanic sequences, they are always interlayered within N-MORBs, as observed in the 900-m-thick volcanic series near Kalur in Albania (see Bortolotti et al., 2002). Moreover, these volcanic sequences are commonly topped by typical SSZ volcanic rocks (IATs or boninites) and are cross cut by boninite dykes, as observed in the Kalur and Kacinar sequences in Albania (Bortolotti et al., 2002; Dilek et al., 2008) and in the Aspropotamos sequence of the Pindos ophiolites in Greece (Jones and Robertson, 1991; Saccani and Photiades, 2004). MTBs are characterized by very strong Th and Nb depletion with respect to other incompatible elements (Fig. 3a), as well as very strong LREE depletion compared to both MREE and HREE (Fig. 3b). When

Table 1
Ophiolitic basaltic rock-types used in this paper, their locations (see also Fig. 1), approximate ages and related data source references. Age abbreviations, Jr: Jurassic; Cr: Cretaceous; Mesoz: Mesozoic; Paleoc: Paleocene; E: Early; L: Late. Rock-type abbreviations, G: garnet-influenced MORB (mid-ocean ridge basalt); N: normal-type MORB; E: enriched-type MORB; P: plume-type MORB; AB: alkaline basalt; MTB: medium-Ti basalt; D: supra-subduction zone depleted-type MORB; IAT: low-Ti, island arc tholeiite; Bon: very low-Ti, boninitic-type basalt; CAB: calc-alkaline basalt; BABB: back arc basin basalt. Other abbreviations, LPL: lower pillow lava; UPL: upper pillow lava; Fm: formation.

Region	Zone/Area	Ophiolite	Age	Basaltic rock-type (number of samples)	Reference
Italy/France	W Alps	Platta	Jurassic	G(2), E(2)	Desmurs et al., 2002
	Apennine	External Liguride	Jurassic	G(8)	Montanini et al., 2008
	Elba Island		Jurassic	G(8)	Author's unpublished data
	Calabria	Calabria	Jurassic	G(7), E(3)	Author's unpublished data
	Corsica	Pineto, Rio Magno	Jurassic	G(2), N(19)	Saccani et al., 2000
		Balagne, Nebbio	Jurassic	G(8) E(5)	Saccani et al., 2008a
		Schistes Lustres	Jurassic	G(22) N(4)	Saccani et al., 2008a
Romania	East Carpathians	Rarau/Hagimas	Triassic	N(6), E(3), AB(7), IAT(2), CAB(4)	Hoeck et al., 2009
	Transylvanian Depression	Zoreni	Jurassic	Bon(1), CAB(20)	Ionescu et al., 2009
	Apuseni Mountains	Apuseni	Jurassic	N(6), E(6)	Saccani et al., 2001
Bohemian Massif	Sudete	Sleza	Paleozoic	N(21)	Floyd et al., 2002
Bulgaria	Rhodope	Mandrica	Jurassic	Bon(8), IAT(6)	Bonev and Stampali, 2008
Dinarides	Central Dinarides	Maljen mélange	Undefined	N(1), E(1), P(2), IAT(4), CAB(3)	Chiari et al., 2011
		Banja	Jurassic	BABB(7), E(3)	Lugovic et al., 1991
		Kopaonik	Jurassic	Bon(7)	Marroni et al., 2004
		Various	Triassic	CAB(14)	Trubelja et al., 2004
		Various	Jurassic	N(12)	Trubelja et al., 1995
		Varda mélange	Undefined	IAT(2), CAB(2)	Author's unpublished data
		N Kozara	Cretaceous	N(4), E(8), AB(3)	Ustaszewski et al., 2009
		N Kozara/Zlatibor	Jr-Cr	N(8), E(5)	Author's unpublished data
Albania	Mirdita	Western Belt	Jurassic	N(5), E(1), MTB(9), Bon(2)	Bortolotti et al., 2002
		Western Belt mélange	Triassic	N(10), E(2)	Bortolotti et al., 2004
		Western Belt mélange	Triassic	N(6), E(1), MTB(1), CAB(1)	Monjoie et al., 2008
		Western Belt mélange	Triassic	N(5), E(1), MTB(1)	Tashko et al., 2009
		Porava	Triassic	N(2), E(3), AB(1)	Bortolotti et al., 2006
		Western Belt	Jurassic	N(9), IAT(20), Bon(6)	Dilek et al., 2008
		S Mirdita	Jurassic	N(2), MTB(1)	Hoeck et al., 2002
		Tropoja mélange	Jurassic	MTB(4), Bon (4)	Author's unpublished data
Greece	Hellenide Ophiolites	Othrys mélange	Undefined	N(5), P(4)	Bortolotti et al., 2008
		Koziakas	Triassic	E(1), AB(6)	Chiari et al., 2012
		Othrys	Triassic	N(4), E(3), AB(6), CAB(2)	Monjoie et al., 2008
		Othrys mélange	Undefined	N(3), AB(1), MTB(4), Bon(5)	Photiades et al., 2003
		Pindos	Jurassic	N(2), Bon(12)	Saccani and Photiades 2004
		Argolis mélange	Undefined	N(6), E(3), P(6), AB(1), Bon(10)	Saccani and Photiades 2005
		Koziakas mélange	Undefined	N(1), E(4), Bon(3)	Saccani et al., 2003a
		Argolis mélange	Triassic	N(4), E(7)	Saccani et al., 2003b
		Almopias melange	Undefined	N(6), E(4), AB(3), Bon(9)	Saccani et al., 2008b
		Guevgueli	L Jurassic	BABB(13), CAB(12)	Saccani et al., 2008c
		Vourinos	Jurassic	IAT(14)	Saccani et al., 2008d
	Attic-Cycladic Zone	Samotraki	Jurassic	BABB(12), CAB(5)	Koglin et al., 2009a,b
		Lesvos mélange	Jurassic	N(5), E(4)	Koglin et al., 2009a,b
		Siphnos	Undefined	CAB(9)	Mocek, 2001
		Kamariza	Undefined	N(1), E(2), P(2), CAB(19)	Photiades and Saccani 2006
Turkey	Izmir-Ankara	Ankara Mélange	L Jr-E Cr	G(3), E(2), AB(8), CAB(2)	Bortolotti et al., 2013
	–	Ankara Mélange	Triassic	E(4), IAT(4), BABB (6)	Göncüoglu et al., 2010
	–	Refahiye	L Cretaceous	IAT(9)	Sarifakioglu et al., 2009
	–	Ankara Mélange	Undefined	N(6), E(7), AB(5), CAB(7)	Tankut et al., 1998
	Antalia	Tekirova	L Cretaceous	AB(2), IAT(8), Bon(6)	Bagci et al., 2006
	Tauride	Kizildag	L Cretaceous	IAT(13), Bon(6)	Dilek and Thy, 2009
		Kizildag	L Cretaceous	IAT(7), CAB(2)	Parlak et al., 2009
	Adana Basin	Misis Ophiolite	Miocene	CAB(10)	Floyd et al., 1991
	Intra-Pontide	Arkotdag Mélange	Jurassic	N(11)	Göncüoglu et al., 2008
	NW Anatolia	Istanbul–Zonguldak	Precambrian	IAT(6), Bon(1), BABB(4)	Yigitbas et al., 2004
Cyprus	Troodos	LPL, UPL	L Cretaceous	IAT(3), Bon(9)	Osozawa et al., 2012
Caucasus	Armenia	Sevan	Cretaceous	BABB(7), AB(10)	Rolland et al., 2009
Iran	Zagros	Baft	Jurassic	N(4), E(4), P(8)	Arvin and Robinson, 1994
		Kermanshah	Triassic	G(4), N(3), E(3), P(17), AB(4)	Saccani et al., 2013b
Iran	Makran	Makran	L Jurassic	E(9)	Ghazi et al., 2004
	Sistan	Nehbandan	undefined	N(4), E(7)	Saccani et al., 2010
	Azerbaijan	Misho	Carboniferous	G(4), E(1), P(13), AB(2)	Saccani et al., 2013a
	S Caspian	S Caspian	L Cretaceous	AB(7), CAB(7)	Salavati, 2008
Oman		Hawasina	Cretaceous	P(12), AB(44)	Chauvet et al., 2011
		Semail	Cretaceous	N(10), E(4)	Einaudi et al., 2000
		Semail	Cretaceous	N(7), IAT(5)	Godard et al., 2006
		Para-authoctonous	Permian	N(5), E(11), AB(15)	Lapierre et al., 2004
India	SW India	Kandra	Paleoproterozoic	E(3), P(3)	Kumar et al., 2010
	Indo-Myanmar	Manipur	Mesoz-Paleoc	N(6), E(7)	Singh et al., 2012
	Palghat-Cauvery SZ	Manamedu	Neoproterozoic	IAT(3), Bon(5), CAB(1)	Yellappa et al., 2010
Tibet	Yarlung Zangbo	Saga	L Jr-E Cr	N(12), P(2), AB(5)	Bedard et al., 2009

(*continued on next page*)

Table 1 (*continued*)

Region	Zone/Area	Ophiolite	Age	Basaltic rock-type (number of samples)	Reference
		Ophiolite Mélange	Jurassic	N(1), E(1), AB(4), SD(1), CAB(2)	Dupuis et al., 2005
		Xigaze	Cretaceous	N(15)	Guilmette et al., 2009
		Zedong	Jurassic	SD(6)	Malpas et al., 2003
		Rembu	Jurassic	AB(16)	Xia et al., 2008
		Zhongba	E Cretaceous	AB(10)	Dai et al., 2011
	Bangong-Nujiang	Bangong Lake	Jurassic	E(8), Bon(8)	Shi et al., 2008
		Lagkor Tso	Jurassic	N(3), E(5), IAT(11), Bon(1)	Wang et al., 2008
	North Qinghai	Buqingshan	Ordovician	N(9)	Bian et al., 2004
	various	various	Jurassic	N(3), E(5)	Xu and Castillo, 2004
	N Tibet	Qintang	undefined	E(9), AB(18)	Zhai et al., 2011
China	NW China	W Junggar	Paleozoic	E(13) AB(6) IAT(2)	Chi et al., 1993
	Qinling-Kunlun	Shangdan	Cambrian	N(18), E(11), Bon(2), CAB(34)	Dong et al., 2011
		A'nyemaqen	Paleozoic	N(10), P(1), AB(8)	Guo et al., 2007
		Mian Lue	Carboniferous	N(6)	Xu et al., 2008
	NW China	Sartuohai	Devonian	E(7), AB(8)	Yang et al., 2012
	SW China	Changning–Menglian	Permian	N(1), IAT(6)	Jian et al., 2009
		Yaxianqiao	Permian	CAB(2)	Jian et al., 2009
		Jinshajiang	Carboniferous	E(14)	Jian et al., 2009
		Ailaoshan	Devonian	N(1)	Jian et al., 2009
	SE China	Jiangxi	Neoproterozoic	N(1), Bon(1), CAB(4)	Li et al., 1997
	Inner Mongolia-Daxinganling	Hegenshan	Permian	N(9), E(6), IAT(3)	Miao et al., 2008
	Kunlun	Kudi	Cambrian	E(2)	Wang et al., 2001
		Kudi	Cambrian	N(8), E(8), IAT(3), BABB(10)	Yuan et al., 2005
	Yunnan	Jinshajiang	Paleozoic	AB(16)	Xiao et al., 2008
	Altay	Kuerti	Paleozoic	SD(1), BABB(13)	Xu et al., 2003
	Alia Shan	Shuanggou	Carboniferous	N(1)	Yumul et al., 2008
	Various	Various	Various	N(4), E(2), Bon(3)	Zhang et al., 2003
Japan	SW Japan	Mino-Tamba	Permian	P(13), AB(5)	Ichiyama et al., 2008
	Hokkaido	Gokurakudaira	L Jurassic	SD(5), CAB(1), BABB(5)	Takashima et al., 2002
Russia	Sikhote-Alin	Moneron-Samarga	Cretaceous	CAB(14)	Malinovsky et al., 2008
	Polar Urals	Enganepe	Neoproterozoic	P(2), IAT(2), Bon(3)	Scarrow et al., 2001
	Kamchatka	E Peninsulas	L Cr-Paleocene	N(12), E(2), BABB(3)	Tsukanov et al., 2007
Australia	New England	Marlborough	Paleozoic	E(7), IAT(2), CAB(1)	Bruce and Niu, 2000
		Marlborough	Neoproterozoic	N(4)	Bruce et al., 2000
		Yarrol	Carboniferous	IAT(9)	Bryan et al., 2001
	New S Wales	Folly basalt	Devonian	N(6), E(4)	Caprarelli and Leitch 2002
		Capertee	Ordovician	CAB(9)	Carr et al., 2003
	Queensland	Gympie Group	Permian-Triassic	CAB(22)	Sivell and McCulloch, 2001
Indonesia	Irian Jaya	Cyclops	Eocene	N(5), Bon(3)	Monnier et al., 1999
	Central Indonesia	Seram-Ambon	Neogene	IAT(4), CAB(2), BABB(6)	Monnier et al., 2003
New Caledonia		Ophiolitic Nappe	L Eocene	N(4), E(11), AB(1)	Cluzel et al., 2001
New Zealand	Northland allochton	Northland	Eocene	N(5), P(1), AB(4), BABB(5)	Thompson et al., 1997
SW Pacific	Macqurie Island		Eocene	E(3), AB(4)	Kamenetsky et al., 2000
Thailand	Nan-Uttaradit	Ophiolite Mélange	Paleozoic	P(10)	Shen et al., 2010
N America	Newfoundland	Betts Cove	Ordovician	Bon(25)	Bédard, 1999
	California	Josephine	Jurassic	IAT(9), Bon(11), BABB(6)	Harper, 2003
		Stonyford	Jurassic	N(1), E(18), AB(11), IAT(2)	Shervais et al., 2005
		Trinity	Paleozoic	IAT(5)	Metcalf et al., 2000
	Canada	Trans-Hudson	Paleoproterozoic	CAB(6), BABB(15)	Maxeiner et al., 2005
		Thetford Mines	Ordovician	IAT(3), Bon(13)	Pagé et al., 2009
	Cascades	Ingalls	Jurassic	N(2), AB(1), IAT(3), CAB(1)	Metzger et al., 2002
Caribbean	Dominican Republic	Los Ranchos	Cretaceous	IAT(9), Bon(5)	Escuder Viruete et al., 2006
		Rio S. Juan	Cretaceous	N(20), IAT(8), Bon(2)	Escuder-Viruete et al., 2011
		Duarte	L Jurassic	N(9)	Lapierre et al., 1999
		Central Dominica	Cretaceous	E(2), AB(1), IAT(2)	Lewis et al., 2002
	Venezuela	Loma de Hierro	L Jr-Cr	N(9), E(2), P(3), IAT(7)	Giunta et al., 2002
	Jamaica	Bath–Dunrobin Fm	Cretaceous	E(17)	Hastie et al., 2008
	Colombia	W Cordillera	Cretaceous	E(5)	Kerr et al., 1996
		W Cordillera	Cretaceous	E(5)	Millward et al., 1984
	Caribbean Plateau	W Cordillera	Cretaceous	N(1), E(3), P(1), AB(1)	Kerr et al., 1998
	Equador	W Cordillera	L Cretaceous	N(32)	Mamberti et al., 2003
		Pinon Fm	Cretaceous	E(10), CAB(1)	Reynaud et al., 1999
	Cuba	Téneme	Cretaceous	N(1), IAT(4), Bon(9)	Proenza et al., 2006
	Costa Rica	S.Elena II, III, IV	E Cretaceous	IAT(3)	Hauff et al., 2000
		S.Elena I-Tortugal	L Cretaceous	AB(8)	Hauff et al., 2000
		Quepos	L Cretaceous	P(8)	Hauff et al., 2000
		Osa	Paleocene	N(3)	Hauff et al., 2000
S America	S Chile	Taitao	L Cretaceous	N(3), CAB(19)	Guivel et al., 2003
Egypt	Central-E Desert	Metavolcanic Fm	Neoproterozoic	IAT(13), BABB(9)	Ali et al., 2009
		Mélange	Neoproterozoic	N(4), E(2), Bon(2), BABB(2)	Farahat, 2010
	E Desert	Fawakir	Neoproterozoic	IAT(33), Bon(3), CAB(6)	El-Rahman et al., 2009
Ethiopia	S Ethiopia	Adola	Neoproterozoic	E(2), Bon(16)	Wolde et al., 1996

compared to N-MORBs, these rocks show slightly lower abundance in P, Hf, Zr, Ti, Y, and MREE/HREE ratios. If compared to IATs, they show similar abundance of P, Hf, Zr, Ti, Y, but slightly higher concentrations of both MREE and HREE. However, the most striking difference between MTBs and IATs is that the former have strong Th depletion, whereas the latter have relative Th enrichment, which is indicative of SSZ-type enrichment by fluids released from the subducting slab (as also observed in boninitic basalts).

Saccani et al. (2011) suggested that primary MTB melts may have derived from partial melting of depleted mantle (cpx-poor lherzolite or cpx-rich harzburgite), which is residual after MORB melt extraction, without the addition of subduction components. According to Bébien et al. (2000), the partial melting of a depleted mantle without a significant contribution from SSZ fluids requires an anomalously high thermal regime. Moreover, the coexistence of MTBs and N-MORBs in the same volcanic section implies that partial meltings of two compositionally distinct mantle sources were contemporaneously active in the same area. Therefore, different authors, though with some variants, postulated that MTBs formed during the early stage of a subduction (nascent forearc) that was established close to a mid-ocean ridge (Bébien et al., 2000; Insergueix-Filippi et al., 2000; Bortolotti et al., 2002; Hoeck et al., 2002; Dilek et al., 2008). In addition, a few basalts from different ophiolitic complexes of various ages show chemical characteristics very similar to those of MTBs. These basalts, beside marked depletion in Th and Nb compared to other HFSE (e.g., Ti, P, Zr, Y) share many geochemical features with MTBs, such as strong depletion in LREE with respect to MREE and HREE and Ti, Zr, Y contents similar to those of N-MORBs. They include Jurassic samples from the ophiolitic mélange (Dupuis et al., 2005) and the Zedong unit (Malpas et al., 2003) in the Yarlung Zangbo suture zone in Tibet, samples from the Paleozoic Kuerti ophiolites in the Altai region (Xu et al., 2003) and from the Jurassic Gokurakudaira (Hokkaido) ophiolites in Japan (Takashima et al., 2002). All these authors described these basalts as MORB-like rocks showing depleted features that originated from depleted mantle sources. In particular, Xu et al. (2003) concluded that these basalts from the Kuerti ophiolites have a geochemical and isotopic signature suggesting a depleted mantle source not significantly modified by the addition of subduction components and that they

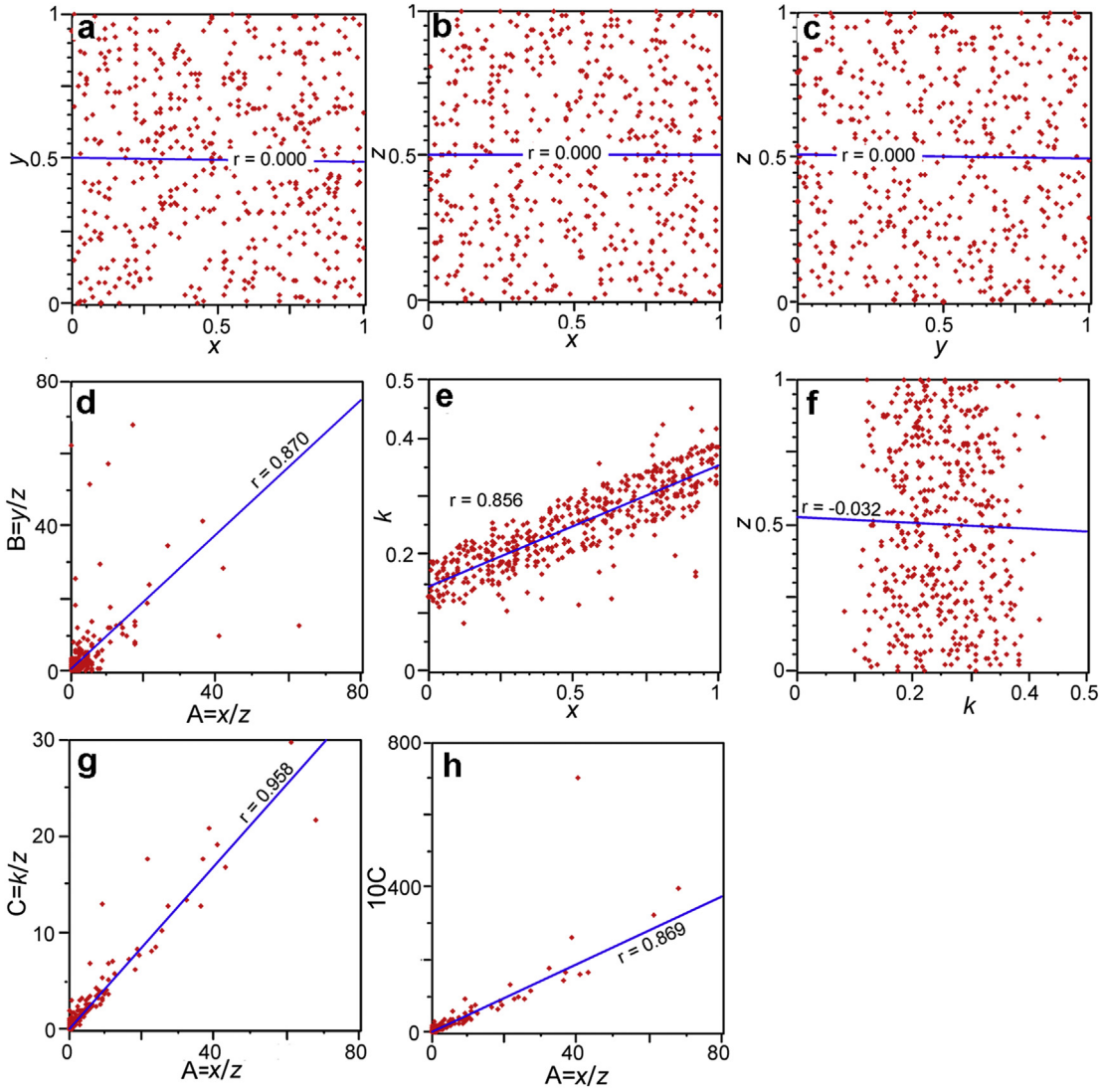

Figure 4. (a–d) Plots of one set of 1500 random numbers used to generate spurious self-correlations for totally uncorrelated variables *x*, *y*, *z*. (e–g) Plots of one set of 1500 random numbers used to generate spurious self-correlations where *k* is correlated with *x*, whereas *x*-*z* and *k*-*z* are uncorrelated. (h) Spurious self-correlations generated for a variable (10C) in the range 0–800 vs. a variable (A) in the range 0–80.

were most likely generated in a back-arc basin setting. Likewise, Takashima et al. (2002) suggested that similar basalts from Hokkaido ophiolites were generated in a SSZ setting, such as fore-arc, intra-arc, or back-arc regions. Although the overall chemistry, as well as the postulated petrogenesis and mantle source compositions of these basalts are very similar to those of MTBs, I prefer to collectively define these rocks as SSZ depleted (D-) MORB, because a definite correspondence between MTBs and these rocks is yet to be proved.

Calc-alkaline basalts (CAB) commonly form in mature, ensimatic volcanic arc settings (e.g., Sierra Nevada, California; Guatemala-Cuba-Venezuela, central America). They are commonly found in volcanic-arc ophiolites, which differ from supra-subduction zone ophiolites based on their thicker and more fully developed arc crust

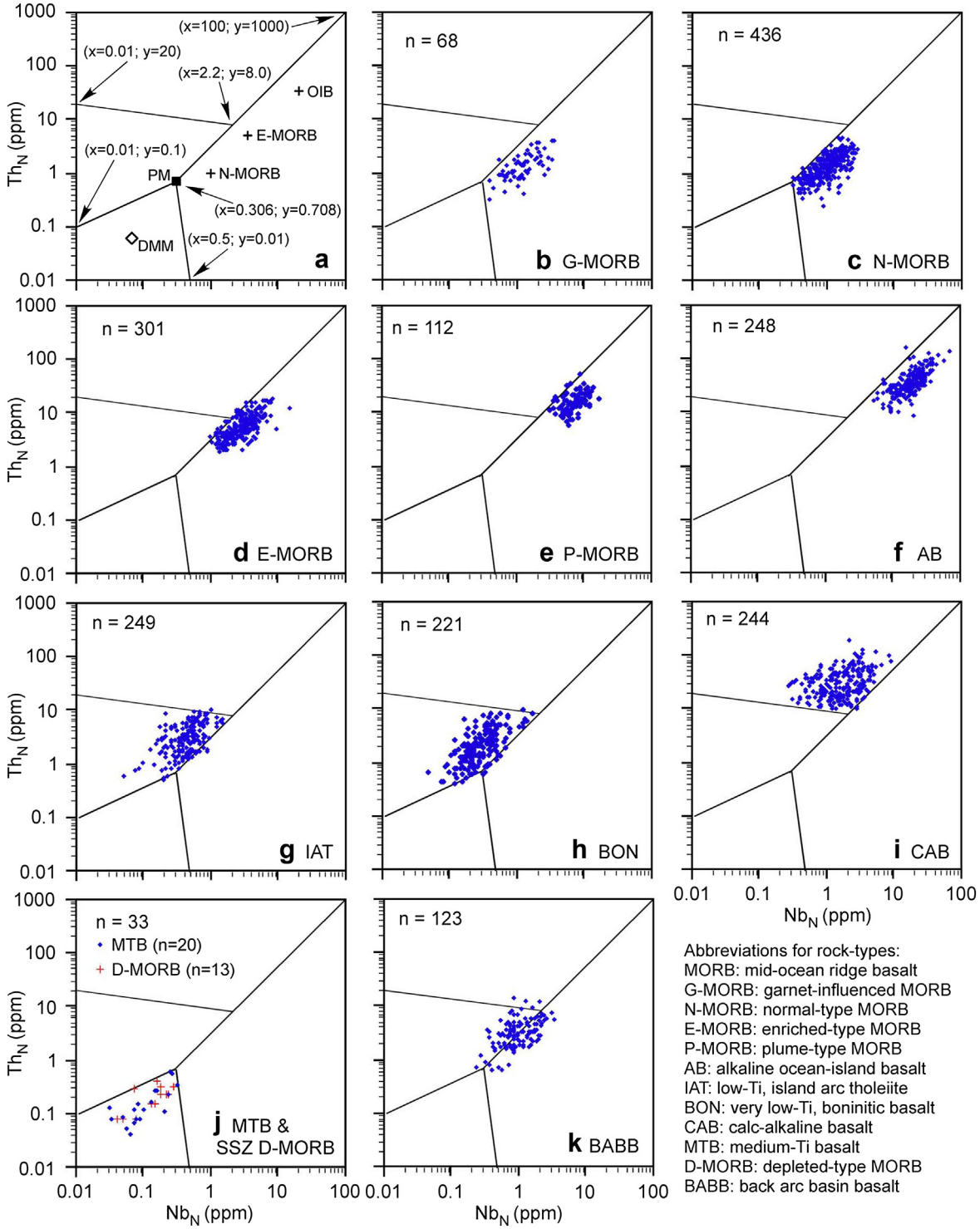

Figure 5. Plots of different post-Archean ophiolitic basaltic rock-types on Th_N vs. Nb_N diagrams. Nb and Th are normalized to the N-MORB composition (Sun and McDonough, 1989). See Table 1 for data sources. The compositions of primordial mantle (PM) and depleted MORB mantle (DMM) shown in panel (a) are from Sun and McDonough (1989) and Workman and Hart (2005), respectively. n = number of samples.

(Dilek and Furnes, 2011). The polygenetic crustal structure of volcanic arc settings (Dilek and Furnes, 2011) largely favors crustal chemical input and wall rock assimilation (e.g., DePaolo, 1981), which result in a significant enrichment in Th and LREE compared to Nb and HREE, respectively. Moreover, these basalts typically show Ta, P, and Ti depletion, which is interpreted to reflect partial melting of depleted mantle sources (e.g., Pearce, 1982).

Backarc basin basalts (BABB) may form in both oceanic and continental backarc basins as a result of seafloor spreading in ensimatic and ensialic settings, respectively (Dilek and Furnes, 2011). They may form in embryonic backarcs (subduction-proximal) that may evolve to mature backarcs (subduction-distal). BABBs commonly derive from partial melting of ascending N-MORB source-like asthenosphere, as a consequence of the backarc rifting (e.g., Taylor and Martinez, 2003; Pearce and Stern, 2006). These basalts may show a large variability in LILE/HFSE (e.g., Th/Tb, Th/Yb, Ta/Yb, Th/Ta, and Ba/Zr) and LREE/HREE ratios, depending on the extent of metasomatic enrichment of the mantle sources by SSZ components.

3. Database

Initially, a database comprising about 2200 geochemical analyses of basaltic rocks from worldwide ophiolitic complexes was compiled from the literature. In order to avoid as much as possible compositional variations due to fractional crystallization processes, only basaltic rock-types were chosen. Moreover, the choice of mafic rock samples was restricted to those ophiolitic complexes for which the tectonic setting of formation was unambiguously described by the author(s). Nonetheless, each of the 2200 samples was checked for the consistency of its tectonic and chemical classification using incompatible elements and REE, as well as a number of well-known tectonic discrimination diagrams used in combination (e.g., Wood, 1980; Pearce, 1982, 2008; Shervais, 1982; Meschede, 1986; Cabanis and Lécolle, 1989). Moreover, ABs have been distinguished from enriched MORB types on the basis of Nb/Y ratios being >1 (Pearce, 1982). For a limited number of samples (about 6%) some discrepancies between the postulated tectonic classification and the chemical analyses were observed. These incongruities were observed mainly in high pressure-low temperature (HP-LT) metamorphic rocks, where mobilization of several elements (including many of those assumed as relatively immobile, see Pearce, 1982) may have obliterated the original geochemistry leading to an objective difficulty in tectonic classification. In a few cases, the inconsistency of the tectonic classification was probably due to poor analytical data. Samples showing ambiguity in their tectonic and chemical classification were excluded and the database used in this paper was then reduced to 2035 samples. Such a number of samples can be considered to be statistically valid and representative of ophiolitic basaltic rocks worldwide. Details on location, age, geochemical affinity, and related references of the samples used herein are summarized in Table 1, whereas their worldwide coverage is presented in Fig. 1. The database includes rocks spanning in age from Proterozoic to Cenozoic. These rocks are mostly represented by volcanic and subvolcanic varieties, though a limited number of gabbros described by the authors as representative of liquid compositions were also included. According to the authors' descriptions, most of the samples are affected by low temperature alteration mainly due to ocean-floor metamorphism. Nonetheless, the database also includes medium- and high-grade metamorphic rocks (up to amphibolite-facies), as well as different varieties of HP-LT metamorphic rocks. Finally, the database includes samples from both coherent volcanic sequences and disrupted sequences incorporated in mélange terranes, regardless of whether or not these sequences match the "ophiolite" definition of the Penrose Conference (Anonymous, 1972). The rationale behind this choice is that the aim of this paper is to include all the possible basaltic types that can be found in ophiolites. Indeed, many rocks incorporated in ophiolites, though not strictly classifiable as "ophiolites" may effectively assist in defining the tectonic evolution of an ancient oceanic basin and surrounding continental margins.

4. Spurious self-correlations using element ratios having a common component

The correlation of two ratios with a common variable was first reported by Pearson (1897) who called such ratio correlations simply "spurious correlations". Kenney (1982) suggested to use the term "spurious self-correlation" for distinguishing the spurious correlation resulting from a common variable from other forms of spurious correlation. Although spurious self-correlation is widely known in biological, sociological, and economics studies (e.g., Kuh and Meyer, 1955; Atchley et al., 1976; Kronmal, 1993), they are generally overlooked by scientists working in earth science disciplines. Chayes (1949) is one of the few authors that brought to the attention of geologists numerous examples of spurious self-correlation in the petrographic literature.

A spurious self-correlation arises when one variable, A (a sum, ratio, or product) is correlated with a second variable, B (a sum, ratio, or product) and the two parameters have some element in common. Given that, the correlation coefficient (r) is a remarkably useful index of the relation between two variables, consider three independent random variables x, y, and z. If x is plotted against y, a scatter graph results and the correlation coefficient r_{xy} between the two variables is equal to zero. Likewise, $r_{xz} = 0$ and $r_{yz} = 0$. However, if two parameters A and B are formed from the original variables, such that $A = x/z$ and $B = y/z$, the correlation coefficient $r_{AB} \neq 0$ (see Kenney, 1982). When A is plotted against B, a line may be fitted to the individual data points. From this line a value of $B = y/z$ can be determined for each value of $A = x/z$. Hence, it would appear that a value of y can be determined from a value of x even though it was initially assumed that all three variables were independent of each other. The correlation coefficient r_{AB} is called spurious because it implies a correlation between two parameters formed from independent variables. The numerical value of the spurious self-correlation coefficient r_{AB} is dependent upon the form of the parameters (sum, ratio, product, etc.) and the variability of each of the original variables. Fig. 4 shows two sets of 1500 random numbers that are used to generate spurious self-correlations. In the first set, three totally independent variables (x, y, and z) are used (Fig. 4a–c). It can be observed that a marked spurious self-correlation is generated when plotting y/z (A) against x/z (B), with $r_{AB} = 0.870$ (Fig. 4d). In the second set of random numbers (right column), the variable k is correlated with x, having $r_{xk} = 0.856$ (Fig. 4e), whereas k and z (Fig. 4f), as well as x and z (Fig. 4b) are mutually independent. In Fig. 4g it can be observed that in this case also a spurious self-correlation is generated when plotting k/z (C) vs. x/z (A), but its influence is definitely lower than that observed for the first set of variables. Moreover, in Fig. 4h it is shown that when plotting the ratio C multiplied by ten (10C) vs. A, the generated spurious self-correlation ($r_{A10C} = 0.869$) differs from that arising in the C vs. A plot ($r_{AC} = 0.958$). Therefore, it should be noted that the spurious self-correlations have very different effects for the two sets of data considered herein. In fact, from the Eqs. (4) and (5) in Chayes (1949) it can be demonstrated that:

- The lesser are r_{xy}, r_{xz}, and r_{yz}, the greater is $r_{(x/z,\ y/z)}$;
- If $r_{xy} >> r_{xz} = r_{yz}$, the influence of spurious self correlation is greatly reduced (or even negligible);

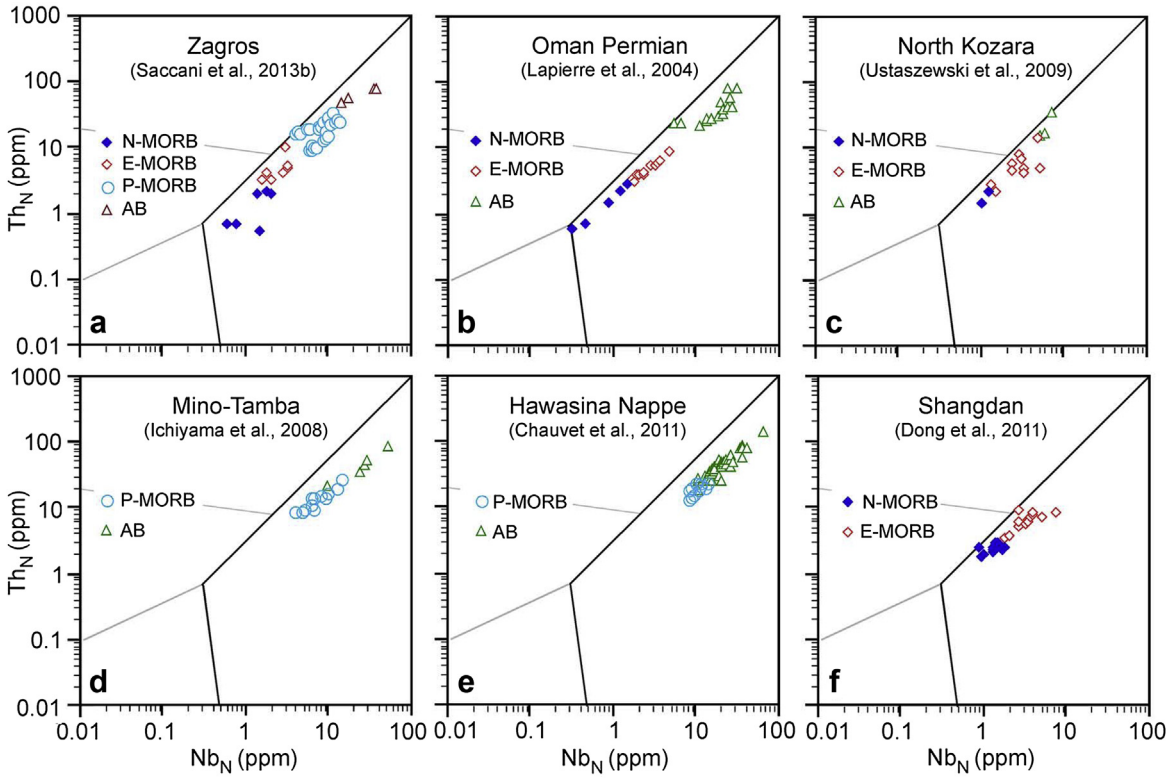

Figure 6. Plots of selected examples of oceanic, subduction-unrelated ophiolitic sequences on Th_N vs. Nb_N diagrams. Nb and Th are normalized to the N-MORB composition (Sun and McDonough, 1989). Fields indicating the compositional variation of different rock varieties are based on Fig. 5. Abbreviations, MORB: mid-ocean ridge basalt, N-: normal type, E-: enriched type, P-: plume type, AB: alkaline basalt.

- When $r_{xy} \neq r_{xz} \neq r_{yz}$, the resulting $r_{(x/z,\ y/z)}$ is variable and unpredictable;
- $r_{(x/z,\ y/z)}$ is strictly depending on the order of magnitude of the variables x, y, z.

The examples shown in Fig. 4 very clearly illustrate well the conclusions of Chayes (1949) that can be summarized as follows:

- using element ratios with a common variable should be avoided;
- the formation of ratios should be confined to those cases in which hypotheses being tested deal with ratios;
- deducing a meaning from ratios (as often observed in literature) is in many cases ambiguous and in a few cases definitely misleading;
- The passage from ratio correlation (e.g., x/z vs. y/z) to inference about relations between absolute measures (i.e., x vs. y) – as also frequently observed in literature – is ambiguous at best and often misleading;
- Absolute measures are always preferable when large numbers of observations must be recorded.

From these conclusions, it results that plotting in one x/z vs. y/z graph different magmatic series (i.e., alkaline, calc-alkaline, etc.) having different (x, y), (x, z), (y, z) correlation coefficients and comparing them to each other is mathematically inconsistent. In fact, different extents of spurious self-correlation will be generated for the different magmatic series in a variable and unpredictable way, then precluding an effective interpretation of their mutual relationships. A thorough mathematical examination of the effects that spurious self-correlations may have on the most common tectonic discrimination diagrams is beyond the scope of this paper. Nonetheless, from the mathematical demonstrations in Chayes (1949) it is clear that, at least from a qualitative point of view, these diagrams are realistically more or less affected by this problem. In light of the conclusions by Chayes (1949), it is not surprising that the Ti/1000 vs. V discrimination diagram proposed by Shervais (1982) rarely fails in correctly classifying data (author's personal experience). Indeed, it is based on absolute measures and hence it is not affected by any mathematical distortion.

5. Discriminating between different ophiolitic basaltic rocks

5.1. Th vs. Nb diagram

Pearce (2008) has demonstrated the importance of two geochemical proxies for the identification and classification of oceanic basalts: (1) the Th–Nb proxy, which is particularly useful in highlighting crustal input and hence demonstrating an oceanic, non-subduction setting; (2) the Ti–Nb proxy for indicating the melting depth. However, in his schemes, Pearce (2008) used Yb as a sort of normalizing value for Nb, Th, and TiO_2 abundances, which may result in severe spurious self-correlations. Indeed, when plotting the data from 2035 known ophiolitic basalts (Table 1) on the Th/Yb vs. Nb/Yb diagram of Pearce (2008), variable rates of misclassification can be observed for different basaltic-types (not shown). Interestingly, the rate of misclassification is high for basalts that should fall in the MORB-OIB array. In detail, 17% of N-MORBs, 31% of E-MORBs, 27% of P-MORBs, and 30% of ABs plot in the field for volcanic arc basalts. Taking MORB-OIB array basalts as a whole, a total of 261 out of 1097 samples (25%) are misclassified. In contrast, the rate of misclassification is very low for SSZ-type (volcanic arc array) basalts (2% for boninites; 0% for IATs and CABs). Nonetheless, the rate of overlapping between SSZ samples, having different

magmatic affinities, is very high for these basalts. For example, 98% of IATs overlap with boninites, whereas 88% of boninites overlap with IATs. Again, 20% of boninites + IATs overlap with CABs, whereas 60% of CABs overlap with IATs and boninites. According to Chayes (1949), it is likely that these considerable rates of misclassification may be related (at least in part) to variable behavior of the spurious self-correlations in the different magmatic series. Indeed, using the data under examination (Table 1), dividing Th and Nb by Yb induces quite different extents of spurious self-correlation in oceanic and volcanic arc rocks, if plotted collectively (not shown). Moreover, the same problem is observed when considering single rock-types (i.e., N-MORB, E-MORB, IAT, boninites, etc.). Nonetheless, Th and Nb are particularly useful for discriminating basalts from different tectonic settings (Pearce, 2008). Therefore, this paper intends to develop the method of Pearce (2008) by using absolute measures of Th and Nb plotted in a simple binary diagram (Fig. 5) in order to avoid unwanted spurious self-correlations. This diagram has been used for plotting 2035 mafic rocks from worldwide ophiolitic complexes (Table 1, Fig. 1). In this diagram, Th and Nb are normalized to the N-MORB composition of Sun and McDonough (1989) in order to have a direct idea of the enrichment or depletion with respect to a well-known rock-type such as N-MORB.

A major point arising from Fig. 5 is that >99% of the analyzed basaltic rocks from oceanic, subduction-unrelated settings plot below the segment between the primordial mantle (PM) composition (Sun and McDonough, 1989) and the point with coordinates $Nb_N = 100$; $Th_N = 1000$ (Fig. 5a) thus defining the N-MORB – OIB array (Fig. 5b–f). In contrast, >99% of subduction-related basaltic rocks (Fig. 5h–j) plot above this segment. In detail, 99% of both G-MORBs and N-MORBs plot at the lower Nb-Th part of the array and have similar Nb and Th contents (Fig. 5b, c). This implies that these two ophiolitic basaltic types cannot be discriminated from each other simply using this diagram. E-MORBs (Fig. 5d) and P-MORBs (Fig. 5e) have Nb and Th contents higher than those of N-MORBs and typically form trends extending along the MORB–OIB array away from the N-MORB composition. AB samples plot at the higher Nb-Th part of the N-MORB-OIB array (Fig. 5f).

From Fig. 5b–f it results that there is large overlap between N-MORB and E-MORBs, as well as E-MORBs and ABs. Moreover, P-MORBs totally overlap with both E-MORBs and ABs. Irrespective of their age and location, there is no relationship between samples that are overlapping. Many of the data used in Fig. 5b–f include basaltic rocks from mélange terranes. These include, for example, the Ankara Mélange in Turkey (Tankut et al., 1998; Sarifakioglu et al., 2014), the Lagkor Tso ophiolite in Tibet (Wang et al., 2008),

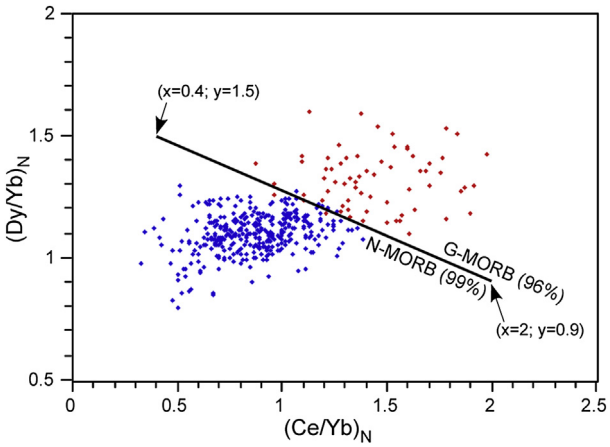

Figure 8. Chondrite-normalized (Sun and McDonough, 1989) Dy/Yb vs. Ce/Yb diagram used for discriminating between G-MORB and N-MORB. The *x*-*y* coordinates of the separation line are given in brackets. In percent are indicated the rates of correct classification using the assumed separation line.

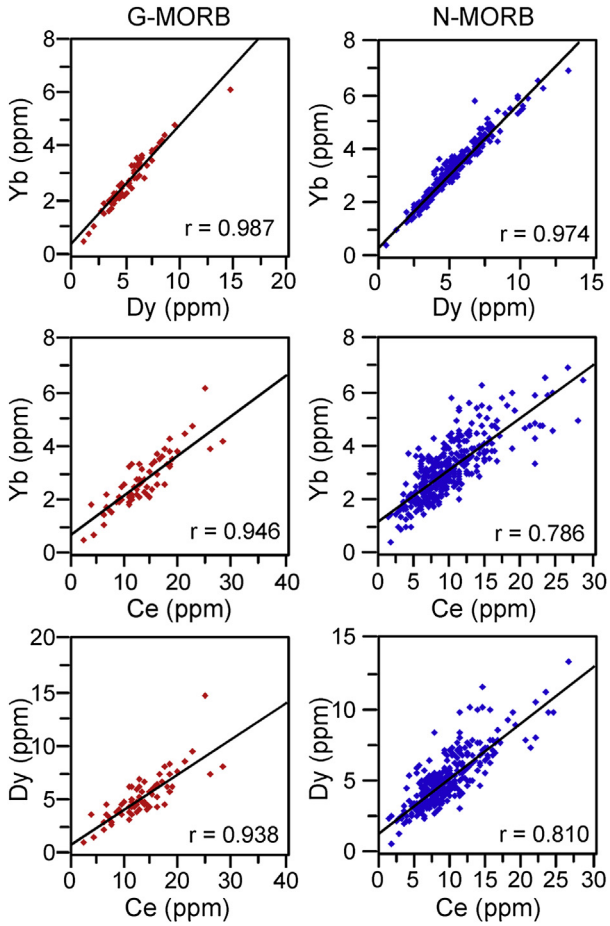

Figure 7. Plots of Dy vs. Yb, Ce vs. Yb, and Ce vs. Dy for G-MORB (garnet-influenced mid-ocean ridge basalt) and N-MORB (normal mid-ocean ridge basalt) rock-types. See Table 1 for data sources.

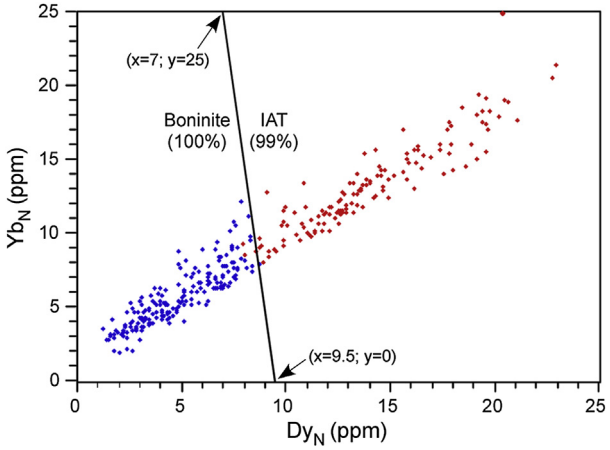

Figure 9. Chondrite-normalized (Sun and McDonough, 1989) Dy vs. Yb diagram used for discriminating between boninitic and IAT (island arc tholeiite) basaltic rocks. The *x*-*y* coordinates of the separation line are given in brackets. In percent are indicated the rates of correct classification using the assumed separation line.

and the New Caledonia ophiolite (Cluzel et al., 2001) where E-MORB samples overlap N-MORB compositions. Nonetheless, overlapping between different basaltic types is also observed in several coherent ophiolitic sequences. Basalts from the Kermanshah ophiolite in Iran (Saccani et al., 2013b), the marginal Permian sequences of Oman (Lapierre et al., 2004), and the North Kozara ophiolites in Bosnia and Herzegovina (Ustaszewski et al., 2009) show the largest chemical variation, which continuously extend

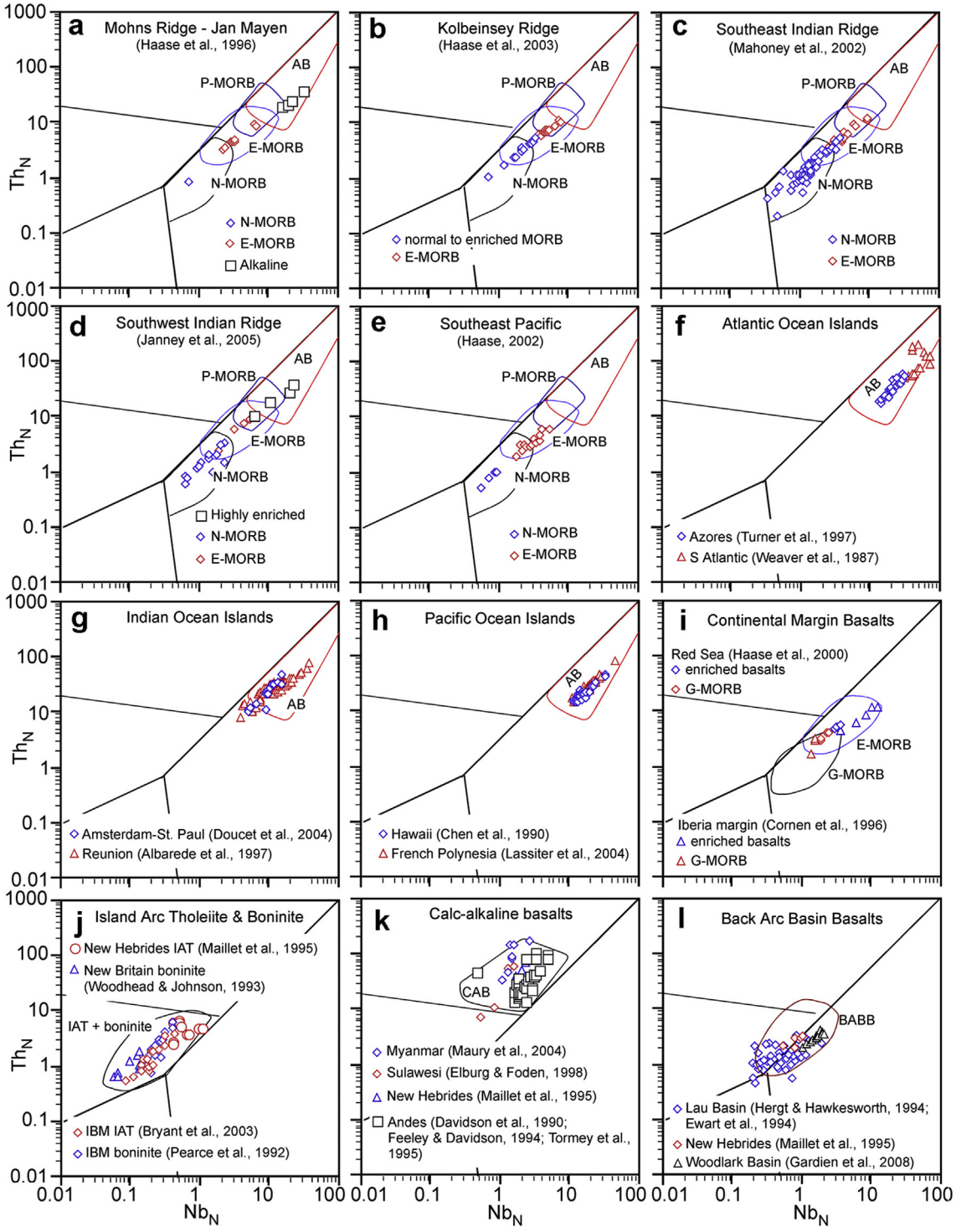

Figure 10. Plots of different basaltic rock-types from modern tectonic settings on N-MORB normalized (Sun and McDonough, 1989) Th vs. Nb diagrams. Locations of samples used and related references are given in each panel. Fields indicating the compositional variation of different rock varieties are based on Fig. 5. Abbreviations, MORB: mid-ocean ridge basalt, N-: normal type, E-: enriched type, P-: plume type, G-: garnet-influenced, AB: alkaline basalt, IAT: island arc tholeiite, CAB: calc-alkaline basalt, BABB: backarc basin basalt (Weaver et al., 1987; Chen et al., 1990; Davidson et al., 1990; Pearce et al., 1992; Woodhead and Johnson, 1993; Ewart et al., 1994; Feeley and Davidson, 1994; Hergt and Hawkesworth, 1994; Maillet et al., 1995; Tormey et al., 1995; Cornen et al., 1996; Haase et al., 1996; Albarède et al., 1997; Turner et al., 1997; Elburg and Foden, 1998; Haase et al., 2000; Haase, 2002; Mahoney et al., 2002; Bryant et al., 2003; Haase et al., 2003; Doucet et al., 2004; Lassiter et al., 2004; Maury et al., 2004; Janney et al., 2005; Gardien et al., 2008).

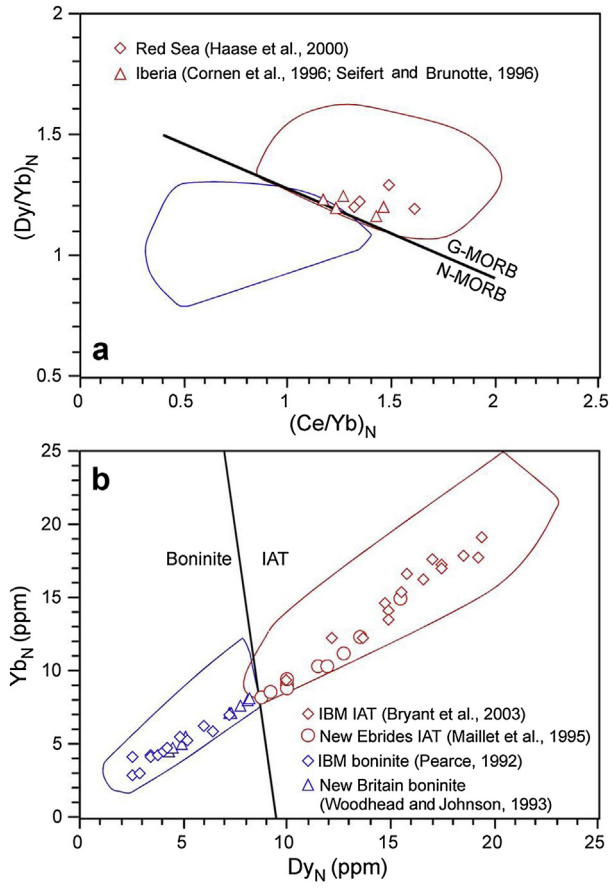

Figure 11. (a) Plot of basalts from modern magma-poor, ocean-continent transitions zones on the chondrite-normalized (Dy/Yb) vs. (Ce/Yb) diagram used for discriminating between G-MORB and N-MORB. (b) Plot of boninitic and IAT (island arc tholeiite) basalts from modern intra-oceanic supra-subduction zone settings on the chondrite normalized Dy vs. Yb diagram. Normalization values are from Sun and McDonough (1989). Locations of samples used and related references are given in each panel. IBM: Izu Bonin Mariana system. Fields indicate the compositional variation of each rock-type, as deduced from Figs. 8 and 9 (Pearce et al., 1992; Woodhead and Johnson, 1993; Maillet et al., 1995; Bryant et al., 2003; Cornen et al., 1996; Haase et al., 2000; Seifert and Brunotte, 1996).

from depleted N-MORB to enriched AB compositions (Fig. 6a–c). Other examples show comparatively limited chemical variations but significant overlapping, as in the Mino-Tamba ophiolites in Japan (Ichiyama et al., 2008) and in the Hawasina Nappe in Oman (Chauvet et al., 2011), where basalts exhibit variable enrichments (Fig. 6d, e), or in the Shangdan ophiolite (Dong et al., 2011) where basalts show N-MORB to E-MORB compositions (Fig. 6f).

Within the SSZ group, IATs and boninites (Fig. 5g, h) plot in the same field, that is above the main division line previously described and below the segment between coordinates ($x = 0.01$; $y = 20$) and ($x = 2.2$; $y = 8$). It is therefore clear that these two ophiolitic basaltic types cannot be discriminated using the Nb-Th systematics. In contrast, CABs (Fig. 5i) can be easily distinguished from IATs and boninites as they plot above the previously defined segment. The misclassification rate for these rocks is <0.5%, as only 1 out of 244 samples plots in the field for MORB-OIB array basalts. CABs used for the present study include both samples from mélange terranes and from coherent volcanic sequences. Typical examples of CABs included in mélange are found in the Dinaride-Albanide-Hellenide ophiolites (Monjoie et al., 2008; Saccani et al., 2008b; Chiari et al., 2011) and in the Ankara and Misis ophiolites in Turkey (Floyd et al., 1991; Tankut et al., 1998; Bortolotti et al., 2013). CABs from coherent volcanic sequences mostly include rocks generated at ensialic volcanic arcs, such as the Jurassic Transylvanian Depression in Romania (Ionescu et al., 2009), Attic-Cycladic zone in Greece (Photiades and Saccani, 2006; Koglin et al., 2009a,b), Guevgueli complex in Greece (Saccani et al., 2008d), Cascades ophiolites in N America (Metzger et al., 2002), as well as the Paleozoic Marlborough Terrane (Bruce and Niu, 2000) and Glympie Group (Sivel and McCulloch, 2001) in Australia and the Bampo Complex (Jian et al., 2009) in the Yaxinqiao ophiolite (SW China).

Medium-Ti basalts and supra-subduction zone depleted MORBs can be readily distinguished from all other ophiolitic rock-types as they plot at the lower Nb-Th part of the diagram (Fig. 5j). Th and Nb contents in these rocks are lower than those of PM (Sun and McDonough, 1989) and, in some cases significantly lower than those of the depleted MORB mantle of Workman and Hart (2005).

Backarc basin basalts from various ophiolitic complexes plot almost symmetrically across the N-MORB-OIB array in the Th_N vs. Nb_N diagram and extend from the PM composition to the lower Th-Nb part of the CAB composition (Fig. 5k). They mainly overlap the Nb-Th compositions of N-MORB, and IAT + boninite. It is therefore clear that a discrimination among these rock-types using Nb-Th systematics is impossible.

5.2. Discriminating between G-MORB and N-MORB: Dy/Yb vs. Ce/Yb diagram

As shown in Section 5.1, G-MORBs and N-MORBs cannot be discriminated using Nb-Th systematics. However, some authors (e.g., Montanini et al., 2008; Saccani et al., 2008a, 2013b) have shown that, in contrast to N-MORBs, G-MORBs show a significant garnet signature. This garnet signature can be highlighted using ratios of LREE/HREE and MREE/HREE, as, for example, Ce/Yb and Dy/Yb. However, using element ratios having a common denominator may result in spurious self-correlations. Nonetheless, it has been shown in Section 4 that spurious self-correlations are negligible when pairs of the three variables used in ratios are strongly correlated to each other. Therefore, the degree of correlation between Ce, Dy, and Yb for both C-MORBs and E-MORBs has been tested and the results are shown in Fig. 7. From this figure, it can be observed that every pair of these three elements for both rock-types shows strong mutual correlations. As a consequence, using Ce/Yb and Dy/Yb ratios for these rocks will not induce any spurious self-correlation. Ce/Yb and Dy/Yb chondrite-normalized (Sun and McDonough, 1989) ratios for G-MORBs and N-MORBs are plotted in Fig. 8. Using these elemental ratios 503 samples of G-MORB and N-MORB can be discriminated from each other. In detail, 96% of the G-MORBs and 99% of the N-MORBs can be discriminated by the segment between coordinates ($x = 2$; $y = 0.9$) and ($x = 0.4$; $y = 1.5$).

5.3. Discriminating between island arc tholeiites and boninites: Yb vs. Dy diagram

As shown in Section 5.1, IATs and boninites cannot be discriminated using Nb-Th diagram. In fact, Pearce (2008) has demonstrated that Th is indicative of subduction input. These rocks largely share the same tectonic environment in intra-oceanic SSZ setting. Therefore, their mantle sources underwent similar Th enrichments prior to melting. Nonetheless, Beccaluva et al. (1984) and Beccaluva and Serri (1988) suggested that boninites originated from higher degrees of partial melting of a depleted mantle source, or, alternatively, from low degrees of partial melting of a more depleted mantle source compared to IATs. Therefore, the search of chemical parameters that can best discriminate between these two rock-types should be addressed to those elements that best account for different degrees of partial melting or different degrees of

depletion of the mantle sources, and should exclude those elements that are related to the subduction-zone contribution to the magma source. To this purpose, exploratory discrimination diagrams, using various combinations of linear and log-transformed trace elements and trace element ratios were performed. However, using element ratios for these rocks always resulted in severe spurious self-correlations (not shown). The best discrimination can then be obtained using absolute measures of Yb and Dy, as shown in the diagram in Fig. 9. These elements indeed better account for different degrees of partial melting and/or different degrees of depletion of the mantle sources. In this diagram, elements are normalized to the chondrite composition (Sun and McDonough, 1989) for the same reasons as explained for the Th-Nb diagram in Fig. 5. Using Yb-Dy systematics, 100% of the analyzed boninites can be discriminated from 99% of IAT by the division line shown in Fig. 9. It should also be noted that the boninitic samples can be discriminated from IAT simply considering the Dy_N value, since 99.5% of boninites have $Dy_N < 8.5$ and 99% of IATs have $Dy_N > 8.5$.

6. Assessment of the results

The discrimination diagrams shown in Section 5 were extremely good at classifying different types of ancient ophiolitic basaltic rocks. From a statistical point of view, as the number of samples in a model increases, its ability to resolve even the smallest subtleties in the data under inspection improves (Vermeesch, 2006). However, the easiest way to obtain a more objective estimate of future performance is to use a second database, which had not been used for the construction of the discrimination diagrams. Therefore, a set of 565 data was compiled from 17 locations (Fig. 1). In order to better assess the consistency of the proposed diagrams, the data from known tectonic settings were used (Fig. 10).

All the oceanic, subduction-unrelated basalts (358 samples) are properly classified within the MORB-OIB array (Fig. 10a–h) and all the subduction-related basalts (120 samples) are perfectly classified in the volcanic arc array (Fig. 10i, j). Nonetheless, within the OIB group, ~5% (10 out of 214 samples), though plot within the MORB-OIB array, occupy outside the compositional field for ABs. All these samples are from the Indian Ocean islands (Fig. 10g). Samples from modern magma-poor, OCTZ (i.e., Iberia and Red Sea–western Arabia rifted margins) include E-MORBs, as well as N-MORBs showing high MREE/HREE ratios (i.e., G-MORBs), which are both accurately classified in the Th-Nb diagram (Fig. 10i). Moreover, G-MORBs are also perfectly distinguished from typical N-MORBs using the $(Ce/Y)_N$ vs. $(Dy/Yb)_N$ diagram (Fig. 11a).

Within the volcanic arc array basalts, all boninite and IAT samples are exactly classified in the IAT + boninite field (Fig. 10i). Using the Yb_N vs. Dy_N discrimination diagram for distinguishing IAT and boninitic basalts (Fig. 11b), all samples from modern oceanic environments are properly classified. The classification of modern CABs using the Th_N vs. Nb_N diagram can also be considered fully satisfactory, as only one out of 60 samples plot outside the CAB field (Fig. 10k). In contrast, 5 out of 87 (~6%) samples of modern BABBs are misclassified (Fig. 10l). All the misclassified samples are from the Lau Basin, whereas samples from the New Hebrides and Woodlark backarc basins are properly classified. In summary, the decision boundaries in the Th_N vs. Nb_N, $(Ce/Y)_N/(Dy/Yb)_N$, and Yb_N vs. Dy_N diagrams seem to perform definitely well for basalts from modern tectonic settings.

7. Critical analysis and limitations of the method

Sections 5 and 6 have shown that the discrimination diagrams proposed in this paper were extremely well at classifying many different types of ancient ophiolitic basaltic rocks, as along with modern rocks from different tectonic settings. Nonetheless, some reflections on the proposed method should be made. The boundary lines in the discrimination diagrams shown in Figs. 5, 8 and 9 were drawn by eye in order to obtain the best discrimination between different basaltic types. In principle, drawing lines by eye is not a statistically rigorous method for discriminating different rock types (see Vermeesch, 2006). Moreover, this conclusion is particularly valid when, once plotted, different populations of samples show

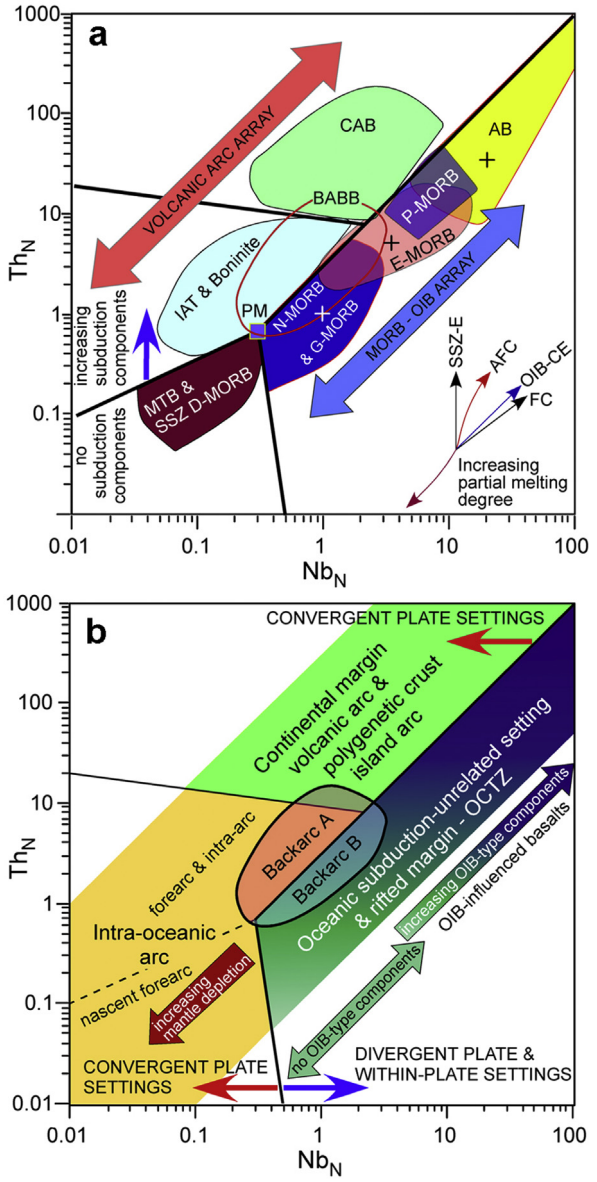

Figure 12. (a) Summary of the compositional variations of different post-Archean ophiolitic basaltic rock-types on the Th_N vs. Nb_N diagram. Vectors indicate the trends of compositional variations due to the main petrogenetic processes. Abbreviations: SSZ-E: supra-subduction zone enrichment; AFC: assimilation-fractional crystallization; OIB-CE: ocean island-type (plume-type) component enrichment; FC: fractional crystallization; other abbreviations as in Fig. 5. Crosses indicate the composition of typical N-MORB, E-MORB and OIB (Sun and McDonough, 1989). (b) Tectonic interpretation of ophiolitic basaltic types based on Th_N-Nb_N systematics. Backarc A indicates backarc basin basalts (BABB) characterized by input of subduction or crustal components (e.g., immature intra-oceanic or ensialic backarcs), whereas Backarc B indicates BABBs showing no input of subduction or crustal components (e.g., mature intra-oceanic backarcs). OCTZ: ocean-continent transition zone. In both panels, Nb and Th are normalized to the N-MORB composition (Sun and McDonough, 1989).

either large overlapping or large gaps. In both these cases, a division line drawn by eye would be absolutely arbitrary. In contrast, the diagrams in Figs. 5, 8 and 9 show that, if oceanic subduction-unrelated rocks are considered collectively, either overlapping or gaps between the different rock groups are negligible. Fig. 12a resumes the chemical variation of all basaltic varieties on the Th_N vs. Nb_N diagram. From this figure it is clear that the chemical distinction between oceanic subduction-unrelated basalts, MTBs, IATs + boninites, and CABs is very sharp. This means that there is very little space for being arbitrary in drawing division lines by eye. Moreover, it should be noted that the triple point separating SSZ basalts with no subduction chemical contribution (i.e., MTB), subduction-related basalts showing subduction chemical contribution (i.e., IAT, boninite, CAB), and MORB-OIB array basalts, which was initially drawn by eye, exactly corresponds to the PM composition. Finally, the major division line discriminating between MORB-OIB array and volcanic arc array basalts is parallel to the line representing the constant ratio between the bulk partition coefficients of Th and Nb calculated for PM composition using the partition coefficients of McKenzie and O'Nions (1991). In fact, Th and Nb behave similarly during partial melting of both spinel-facies and garnet-facies mantle sources for melting degrees higher than 0.5%. Therefore, this boundary line discriminates between basalts generated from mantle sources having Th/Nb ratios higher than that of PM ($Th_N/Nb_N = 2.31$) and basalts generated from mantle sources having Th/Nb ratios lower than that of PM.

It should however be remarked that, as in other discrimination schemes, the method proposed herein shows some limitations. The first limitation is that this method does allow discrimination between basalts generated by shallow (i.e., spinel-facies mantle) or deep (i.e., garnet-facies mantle) melting to be made due to similar behavior by Th and Nb during partial melting in both spinel-facies and garnet-facies mantle sources. For an appropriate recognition of the melting depth, the Ti enrichment relative to garnet-compatible Yb provides an excellent proxy for depth of melting (Pearce, 2008).

Another limitation is that this method does not allow a clear discrimination between different basaltic types within the MORB-OIB array. In fact, Fig. 12a shows that there is large overlapping between N-MORBs and E-MORBs, and between E-MORBs, P-MORBs, and ABs. This limitation may be related to some potential issues. There are some examples of ophiolitic complexes and modern oceanic analogs in which the Th-Nb, as well as REE concentrations extend without interruption from depleted N-MORB to enriched alkaline OIB compositions, as, for example in the Zagros (Iran) ophiolites (Saccani et al., 2013b), in the Permian para-autochthonous sequences of Oman (Lapierre et al., 2004) (Fig. 6a, b) and in the modern Mohns Ridge – Jan Mayen system (Haase et al., 1996) (Fig. 10a). Other examples of ophiolitic complexes and modern oceanic settings showing limited but typical trends from less enriched to more enriched compositions are shown in Fig. 6d–f and Fig. 10e, g. Many authors attribute such trends to mixing of enriched and depleted mantle reservoirs (e.g. Schilling, 1973; Thirlwall et al., 2004), whereas other authors attribute them to loss of melt fractions during the decompression that accompanies asthenospheric flow from an off-axis plume to a ridge (Niu et al., 1999; Phipps Morgan and Morgan, 1999; Pearce, 2005). Finally, Th and Nb behave similarly during both partial melting and fractional crystallization processes (see trends in Fig. 12a). Therefore, Th-Nb compositions of slightly fractionated basalts deriving from comparatively less enriched primary melts originated from a low degree of partial melting, will inevitably overlap with Th-Nb compositions of primitive basalts originated from a high degree of partial melting of a relatively more enriched source. In summary, several petrogenetic factors do not allow the different basaltic types from oceanic subduction-unrelated settings to be clearly discriminated. An accurate examination of several chemical parameters, such as incompatible elements and REE is required to correctly recognize these basaltic types.

A further limitation of the method proposed in this paper is that it does not allow BABBs to be discriminated from some other basaltic types (Fig. 12a). Also this limitation is related to some potential issues. Indeed, BABBs show high variability in terms of incompatible elements and REE, as they may form in a variety of tectonic environments ranging from embryonic to mature backarc and from oceanic to continental (ensialic) settings (Dilek and Furnes, 2011). These different tectonic environments are associated with compositionally different mantle sources, as well as different subduction inputs or crustal contaminations. According to many authors (e.g., Taylor and Martinez, 2003; Pearce and Stern, 2006), the mantle source of BABBs is generally represented by N-MORB-like asthenosphere that may be variably enriched in LILE and LREE by crustal input via subduction or crustal contamination. Therefore, in immature intra-oceanic and ensialic backarcs the erupted basalts will commonly be characterized by crustal chemical influence (e.g., Th enrichment relative to Nb) producing a shift towards high Th compositions. In contrast, basalts from mature backarcs generally show compositions very similar (or virtually undistinguishable) to those of N-MORBs. In order to correctly identify these basalts other geochemical parameters and especially geological data should be used in combination. However, once the backarc nature of basalts is established, the Th_N vs. Nb_N diagram (Fig. 12a) may be very useful for recognizing the possible contribution of subduction or crustal components on their mantle source.

8. Tectonic interpretation

The tectonic interpretation of ophiolitic basalts based on Th-Nb systematics is shown in Fig. 12b. Using these elements, basalts generated at divergent plate and within-plate settings can effectively be distinguished from basalts generated at convergent plate settings. The divergent plate and within-plate settings include oceanic, subduction-unrelated environments, such as mid-ocean ridge spreading centres, oceanic plateaux, and seamounts, as well as incipient oceans at volcanic, non-volcanic (Alpine-type), and transitional rifted margins and/or OCTZ. The Th_N vs. Nb_N diagram highlights the chemical variability of basalts generated in these settings, which range from depleted compositions (N-MORB and G-MORB) to progressively more enriched compositions (E-MORB and P-MORB) and highly enriched compositions (AB). This chemical variation reflects the source composition and degree of melting. Since Th and Nb are insensitive to partial melting of garnet-bearing sources, the recognition of G-MORBs, which are indicative of Alpine-type (Iberia-type) rifted margins and/or OCTZ, can be made using the diagram in Fig. 8.

Based on modern oceanic settings, Pearce (2008) suggested that N-MORBs formed at plume-distal ridge settings, whereas E-MORBs and P-MORBs formed at plume-proximal ridge settings. Likewise, based on combined observations of the internal structure, geochemistry and emplacement modes of ophiolites, Dilek and Furnes (2011) suggested that enriched MORB compositions are indicative of plume-proximal or plume-type ophiolites. However, it should be noted that based only the geochemistry of basalts, the concepts of "plume-proximal" and "plume-distal" cannot be unambiguously applied to ancient ophiolites. Unfortunately, using only geochemical evidence, enriched basalts generated at plume-proximal settings are hard to be distinguished from similar rocks generated at plume-distal settings. The plume-type signature of basalts formed at plume-distal settings may be associated with complex mantle heterogeneities, or chemical features inherited from previous tectonic events, or very low partial melting degree of a depleted mantle source (or, eventually, a combination of these). A

typical example is represented by the Triassic E-MORBs, P-MORBs and ABs (namely, OIBs) that are found in the Dinaride-Hellenide Neo-Tethyan ophiolites (Saccani and Photiades, 2005; Bortolotti et al., 2008; Monjoie et al., 2008; Tashko et al., 2009). In spite of the enriched nature of these rocks, no geological evidence (e.g., regional doming, anomalous thermal regime, oceanic basaltic plateaus, etc.) supporting the existence of a mantle plume activity in that area during Triassic times has so far been documented. In contrast, some authors, using geochemical and isotopic data, have suggested that the mantle sources of the Dinaride-Hellenide Triassic basalts have enriched characteristics that were inherited from previous (Permian?) events (e.g., Pe-Piper, 1998). However, Triassic enriched basalts from the Dinaride-Hellenide ophiolites are chemically undistinguishable from similar rocks that were clearly associated with mantle plume activity (i.e., plume-proximal), such as those generated in the Paleo-Tethyan domain (e.g., Dai et al., 2011; Saccani et al., 2013a) and in the Cretaceous northern Neo-Tethyan basin (see Rolland et al., 2009, and references therein).

In summary, when using a geochemical approach, a distinction of different basalts based on "chemical components" should be preferred, regardless of the tectonic setting in which they were generated. Hence, the use of the more prudential term "OIB-influenced basalts" (OIB-influenced ophiolites) instead of plume-proximal basalts (or ophiolites) is preferred in this paper (Fig. 12b). The OIB term is used here merely for indicating a type of chemical component. As a consequence, the present scheme also enables interaction of OIB-type and typical MORB-type sources (OIB-MORB source interaction) to be identified. Additional evidence is needed to establish if OIB-influenced ophiolites are associated with a real mantle plume activity or mantle source enrichment of a different nature.

Three different types of convergent plate settings can be discriminated on the Th_N vs. Nb_N diagram in Fig. 12b. Island arcs with complex polygenetic crustal nature are largely characterized by the occurrence of CABs, which are displaced to the highest Th-Nb values. Intra-oceanic arcs display a large variability in Th-Nb contents, which can be used for recognizing two sub-types of intra-oceanic arc basalts. The Th/Nb enrichment indicates subduction-mantle source interaction, whereas decreasing Th-Nb compositions with respect to that of PM define an array of mantle depletion without contribution from subduction-derived components (Fig. 12a, b). IATs and boninites are indicative of intra-oceanic arc settings characterized by a variable contribution from subduction-derived chemical components, such as forearc and intra-arc. In contrast, MTBs and SSZ D-MORBs are indicative of intra-oceanic arc settings characterized by no contribution from subduction-derived chemical components, such as nascent forearc (Bébien et al., 2000; Insergueix-Filippi et al., 2000; Bortolotti et al., 2002; Hoeck et al., 2002; Dilek et al., 2008) and, possibly, backarc-proximal intra-oceanic arc settings (see Xu et al., 2003).

Basalts formed in backarc basin settings cannot be straightforwardly identified using Th_N vs. Nb_N systematics. For these rocks there remains considerable ambiguity since they show the highest variability in terms of incompatible elements and REE, as they may form in a variety of tectonic environments ranging from embryonic to mature backarc and from oceanic to continental (ensialic) settings (Dilek and Furnes, 2011). Additional geochemical and, especially, geological constraints need to be used. Nonetheless, the Th_N vs. Nb_N diagram (Fig. 12b) may assist in the recognition of backarc settings characterized by a variable contribution from crustal chemical components (i.e., immature intra-oceanic or ensialic backarcs) and backarcs showing no input of crustal components (e.g., mature intra-oceanic backarcs).

9. Conclusions

In this paper, the method based on the Th-Nb proxy proposed by Pearce (2008) is developed and applied to post-Archean ophiolites in order to provide a new method for the identification of ten different types of ophiolitic basalts and their tectonic setting. The conclusions can be summarized as follows:

(1) A simple N-MORB normalized Th_N vs. Nb_N diagram is proposed as the main discrimination diagram. Using absolute measures plotted in a binary diagram instead of using element ratios or triangular diagrams have the great advantage that unpredictable mathematical artifacts are avoided (Chayes, 1949).
(2) In the Th_N vs. Nb_N diagram, basalts generated in oceanic, subduction-unrelated settings, rifted margins and ocean-continent transition zones are distinguished from subduction-related basalts with a misclassification rate $<1\%$.
(3) The Th_N vs. Nb_N diagram highlights the chemical variance of oceanic, rifted margin, and OCTZ basalts from depleted compositions (N-MORB) to progressively more enriched compositions (E-MORB and P-MORB) and highly enriched compositions (AB), which reflects the variance of source composition and degree of melting.
(4) Within the subduction-related group, basalts formed at island arc with complex polygenetic crust (volcanic arc ophiolites of Dilek and Furnes, 2011) can be distinguished from basalts generated in intra-oceanic island arcs (SSZ ophiolites of Dilek and Furnes, 2011) with a misclassification rate $<1\%$. Within the intra-oceanic arc group, island arc tholeiites and boninites can be distinguished from medium-Ti basalts and SSZ depleted MORBs with a misclassification rate $<0.5\%$. This implies that forearc and intra-arc sub-settings can be discriminated from nascent forearc sub-settings. Moreover, a chondrite-normalized Dy_N-Yb_N diagram is proposed for discriminating between boninite and IAT basalts with a confidence level $>99.5\%$.
(5) A chondrite-normalized $(Ce/Yb)_N$ vs. $(Dy/Yb)_N$ diagram is proposed for discriminating a sub-type of N-MORBs showing a garnet signature (G-MORB), which is generated in Alpine-type (Iberia-type) continental rifts and OCTZ, from typical N-MORBs with a confidence level $>96\%$.

Acknowledgments

The author is very grateful to the staff of the petrology lab of the Ferrara University (particularly to C. Bonadiman), as well as to S. O'Reilly and B. Griffin (GEMOC, Macquarie University, Australia), A. Montanini (Parma University), and M. Marroni (Pisa University) for their fruitful comments on the early version of the manuscript. Many thanks go to G. Xhixha and M. Shyti for their help with mathematics. Y. Dilek and an anonymous reviewer are greatly acknowledged for their constructive reviews of this paper.

References

Agrawal, S., 1999. Geochemical discrimination diagrams: a simple way of replacing eye-fitted boundaries with probability-based classifier surfaces. Journal of the Geological Society of India 54, 335–346.
Agrawal, S., Guevara, M., Verma, S.P., 2008. Tectonic discrimination of basic and ultrabasic volcanic rocks through log-transformed ratios of immobile trace elements. International Geology Review 50, 1057–1079. http://dx.doi.org/10.2747/0020-6814.50.12.1057.
Albarède, F., Luais, B., Fitton, J.G., Semet, M.P., Kaminski, E., Upton, B.G.J., Bachèlery, P., Cheminée, J.-L., 1997. The geochemical regimes of Piton de la Fournaise Volcano (Réunion) during the last 530,000 years. Journal of Petrology 38, 171–201.
Ali, K.A., Stern, R.J., Manton, W.I., Kimura, J.-I., Khamees, H.A., 2009. Geochemistry, Nd isotopes and U-Pb SHRIMP zircon dating of Neoproterozoic volcanic rocks

from the Central Eastern Desert of Egypt: new insights into the ~750 Ma crust-forming event. Precambrian Research 171, 1–22.
Anonymous, 1972. Penrose field conference on Ophiolites. Geotimes 17, 24–25.
Arvin, M., Robinson, P., 1994. The petrogenesis and tectonic settino of lavas from the Baft ophiolitic melange, southwest of Kerman, Iran. Canadian Journal of Earth Sciences 31, 824–834.
Atchley, W.R., Gaskins, C.T., Anderson, D., 1976. Statistical properties of ratios. I. Empirical results. Systematic Zoology 25, 137–148.
Bagci, U., Parlak, O., Hoeck, V., 2006. Geochemical character and tectonic environment of ultramafic to mafic cumulate rocks from the Tekirova (Antalya) ophiolite (southern Turkey). Geological Journal 41, 193–219.
Bébien, J., Dimo-Lahitte, A., Vergély, P., Insergueix-Filippi, D., Dupeyrat, L., 2000. Albanian ophiolites. I – magmatic and metamorphic processes associated with the initiation of a subduction. Ofioliti 25, 39–45.
Beccaluva, L., Serri, G., 1988. Boninitic and low-Ti subduction-related lavas from intraoceanic arc-backarc systems and low-Ti ophiolites: a reappraisal of their petrogenesis and original tectonic setting. Tectonophysics 146, 291–315.
Beccaluva, L., DiGirolamo, P., Macciotta, G., Morra, V., 1983. Magma affinities and fractionation trends in ophiolites. Ofioliti 8, 307–324.
Beccaluva, L., Ohnenstetter, D., Ohnenstetter, M., Paupy, A., 1984. Two magmatic series with island arc affinities within the Vourinos ophiolite. Contributions to Mineralogy and Petrology 85, 253–271.
Beccaluva, L., Chinchilla-Chaves, A.L., Coltorti, M., Giunta, G., Siena, F., Vaccaro, C., 1999. Petrological and structural significance of the Santa Elena-Nicoya ophiolitic complex in Costa Rica and geodynamic implications. European Journal of Mineralogy 11, 1091–1107.
Bédard, J.H., 1999. Petrogenesis of boninites from the Betts Cove Ophiolite, Newfoundland, Canada: identification of subducted source components. Journal of Petrology 40, 1853–1889.
Bédard, J.H., Hébert, R., Guilmette, C., Lesage, G., Wang, C.S., Dostal, J., 2009. Petrology and geochemistry of the Saga and Sangsang ophiolitic massifs, Yarlung Zangbo Suture Zone, Southern Tibet: evidence for an arc–back-arc origin. Lithos 113, 48–67.
Bian, Q.-T., Li, D.-H., Pospelov, I., Yin, L.-M., Li, H.-S., Zhao, D.-S., Chang, C.-F., Luo, X.-Q., Gao, S.-L., Astrakhantsev, O., Chamov, N., 2004. Age, geochemistry and tectonic setting of Buqingshan ophiolites, North Qinghai-Tibet Plateau, China. Journal of Asian Earth Sciences 23, 577–596.
Bonev, N., Stampali, G., 2008. Petrology, geochemistry and geodynamic implications of Jurassic island arc magmatism as revealed by mafic volcanic rocks in the Mesozoic low-grade sequence, eastern Rhodope, Bulgaria. Lithos 100, 210–233. http://dx.doi.org/10.1016/j.lithos.2007.06.019.
Bortolotti, V., Kodra, A., Marroni, M., Mustafa, F., Pandolfi, L., Principi, G., Saccani, E., 1996. Geology and petrology of ophiolitic sequences in the central Mirdita region (northern Albania). Ofioliti 21, 3–20.
Bortolotti, V., Marroni, M., Pandolfi, L., Principi, G., Saccani, E., 2002. Interaction between mid-ocean ridge and subduction magmatism in Albanian ophiolites. Journal of Geology 110, 561–576.
Bortolotti, V., Chiari, M., Kodra, A., Marcucci, M., Mustafa, F., Principi, G., Saccani, E., 2004. New evidence for Triassic MORB magmatism in the northern Mirdita Zone ophiolites (Albania). Ofioliti 29, 243–246.
Bortolotti, V., Chiari, M., Kodra, A., Martucci, M., Marroni, M., Mustafa, F., Prela, M., Pandolfi, L., Principi, G., Saccani, E., 2006. Triassic MORB magmatism in the southern Mirdita zone (Albania). Ofioliti 31, 1–9.
Bortolotti, V., Chiari, M., Marcucci, M., Photiades, A., Principi, G., Saccani, E., 2008. New geochemical and age data on the ophiolites from the Othrys area (Greece): implication for the Triassic evolution of the Vardar ocean. Ofioliti 33, 135–151.
Bortolotti, V., Chiari, M., Göncüoglu, M.C., Marcucci, M., Principi, G., Tekin, U.K., Saccani, E., Tassinari, R., 2013. Age and geochemistry of basalt-chert associations in the ophiolitic complexes of the Izmir-Ankara Mélange East of Ankara, Turkey: preliminary data. Ofioliti 38, 157–173. http://dx.doi.org/10.4454/ofioliti.v38i2.424.
Bruce, M.C., Niu, Y., 2000. Evidence for Palaeozoic magmatism recorded in the Late Neoproterozoic Marlborough ophiolite, New England Fold Belt, central Queensland. Australian Journal of Earth Sciences 47, 1065–1076.
Bruce, M.C., Niu, Y., Harbort, T.A., Holcombe, R.J., 2000. Petrological, geochemical and geochronological evidence for a Neoproterozoic ocean basin recorded in the Marlborough terrane of the northern New England Fold Belt. Australian Journal of Earth Sciences 47, 1053–1064.
Bryan, S.E., Holcombe, R.J., Fielding, C.R., 2001. Yarrol terrane of the northern New England Fold Belt: forearc or backarc? Australian Journal of Earth Sciences 48, 293–316.
Bryant, C.J., Arculus, R.J., Eggins, S.M., 2003. The geochemical evolution of the Izu-Bonin arc system: a perspective from tephras recovered by deep-sea drilling. Geochemistry, Geophysics, Geosystems 4 (11), 1094. http://dx.doi.org/10.1029/2002GC000427.
Cabanis, B., Lécolle, M., 1989. Le diagramme La/10, Y/15, Nb/8: un outil pour la discrimination des séries volcaniques et la mise en évidencedes processus de mélange et/ou contamination crustale. Comptes Rendus de l'Academie des Sciences de Paris 309, 2023–2029.
Caprarelli, G., Leitch, E.C., 2002. MORB-like rocks in a Palaeozoic convergent margin setting, northeast New South Wales. Australian Journal of Earth Sciences 49, 367–374.
Carr, P.F., Fergusson, C.L., Pemberton, J.W., Colquhoun, G.P., Murray, S.I., Watkins, J., 2003. Late Ordovician island-arc volcanic rocks, northern Capertee Zone, Lachlan Fold Belt, New South Wales. Australian Journal of Earth Sciences 50, 319–330.
Chauvet, F., Lapierre, H., Maury, R.C., Bosch, D., Basile, C., Cotten, J., Brunet, P., Campillo, S., 2011. Triassic alkaline magmatism of the Hawasina Nappes: post-breakup melting of the Oman lithospheric mantle modified by the Permian Neotethyan Plume. Lithos 122, 122–136. http://dx.doi.org/10.1016/j.lithos.2010.12.006.
Chayes, F., 1949. On ratio correlation in petrography. Journal of Geology 57, 237–254.
Chen, C.-Y., Frey, F.A., Garcia, M.O., 1990. Evolution of alkalic lavas at Haleakala volcano, East Maui, Hawaii: major, trace element, and isotopic constraints. Contributions to Mineralogy and Petrology 105, 197–218.
Chi, Z., Mingguo, Z., Allen, M.B., Saunders, A.D., Guang-Rei, W., Xuan, H., 1993. Implications of Palaeozoic ophiolites from Western Junggar, NW China, for the tectonics of central Asia. Journal of the Geological Society of London 150, 551–561.
Chiari, M., Djeriç, N., Garfagnoli, F., Hrvatovic, H., Krstiç, M., Levi, N., Malasoma, A., Marroni, M., Menna, F., Nirta, G., Pandolfi, L., Principi, G., Saccani, E., Stojadinoviç, U., Triviç, B., 2011. The geology of the Zlatibor-Maljen area (Western Serbia): a geotraverse across the Dinaric-Hellenic collisional belt. Ofioliti 36, 139–166.
Chiari, M., Bortolotti, V., Marcucci, M., Photiades, A., Principi, G., Saccani, E., 2012. Radiolarian biostratigraphy and geochemistry of the Koziakas massif ophiolites (Greece). Bulletin de la Societé géologique de France 183, 289–309.
Cluzel, D., Aitchison, J.C., Picard, C., 2001. Tectonic accretion and underplating of mafic terranes in the Late Eocene intraoceanic fore-arc of New Caledonia (Southwest Pacific): geodynamic implications. Tectonophysics 340, 23–59.
Cornen, G., Beslier, M.-O., Girardeau, J., 1996. Petrology of the mafic rocks cored in the Iberia Abyssal Plain. In: Whitmarsh, R.B., Sawyer, D.S., Klaus, A., Masson, D.G. (Eds.), Proceedings of the Ocean Drilling Program, Scientific Results, College Station, TX, Ocean Drilling Program, vol. 149, pp. 449–469. http://dx.doi.org/10.2973/odp.proc.sr.149.220.1996.
Dai, J., Wang, C., Hébert, R., Li, Y., Zhong, H., Guillaume, R., Bezard, R., Wei, Y., 2011. Late Devonian OIB alkaline gabbro in the Yarlung Zangbo Suture Zone: Remnants of the Paleo-Tethys? Gondwana Research 19, 232–243. http://dx.doi.org/10.1016/j.gr.2010.05.015.
Davidson, J.P., McMillan, N.J., Moorbath, S., Worner, G., Harmon, R.S., Lopez-Escobar, L., 1990. The Nevados de Payachata volcanic region (18° S/69° w, N.Chile) II. Evidence for widespread crustal involvement in Andean magmatism. Contributions to Mineralogy and Petrology 105, 412–432.
DePaolo, D.J., 1981. Trace Element and isotopic effects of combined wallrock assimilation and fractional crystallization. Earth and Planetary Science Letters 53, 189–202.
Desmurs, L., Muntener, O., Manatschal, G., 2002. Onset of magmatic accretion within a magma-poor rifted margin: a case study from the Platta ocean-continent transition, eastern Switzerland. Contributions to Mineralogy and Petrology 144, 365–382. http://dx.doi.org/10.1007/s00410-002-0403-4.
Dilek, Y., Furnes, H., 2011. Ophiolite genesis and global tectonics: geochemical and tectonic fingerprinting of ancient oceanic lithosphere. Geological Society of America Bulletin 123, 387–411. http://dx.doi.org/10.1130/B30446.1.
Dilek, Y., Thy, P., 2009. Island arc tholeiite to boninitic melt evolution of the Cretaceous Kizildag (Turkey) ophiolite: model for multi-stage early arc-forearc magmatism in Tethyan subduction factories. Lithos 113, 68–87. http://dx.doi.org/10.1016/j.lithos.2009.05.044.
Dilek, Y., Furnes, H., Shallo, M., 2008. Geochemistry of the Jurassic Mirdita Ophiolite (Albania) and the MORB to SSZ evolution of a marginal basin oceanic crust. Lithos 100, 174–209. http://dx.doi.org/10.1016/j.lithos.2007.06.026.
Dong, Y., Zhang, G., Hauzenberger, C., Neubauer, F., Yang, Z., Liu, X., 2011. Palaeozoic tectonics and evolutionary history of the Qinling orogen: evidence from geochemistry and geochronology of ophiolite and related volcanic rocks. Lithos 122, 39–56. http://dx.doi.org/10.1016/j.lithos.2010.11.011.
Doucet, S., Weis, D., Scoates, J.S., Debaille, V., Giret, A., 2004. Geochemical and Hf–Pb–Sr–Nd isotopic constraints on the origin of the Amsterdam-St. Paul (Indian Ocean) hotspot basalts. Earth and Planetary Science Letters 218, 179–195.
Dupuis, C., Hèbert, R., Dubois-Coté, V., Wang, C.S., Li, Y.L., Li, Z.J., 2005. Petrology and geochemistry of mafic rocks from mélange and flysch units adjacent to the Yarlung Zangbo Suture Zone, southern Tibet. Chemical Geology 214, 287–308. http://dx.doi.org/10.1016/j.chemgeo.2004.10.005.
Einaudi, F., Pezard, P.A., Cochemé, J.-J., Coulon, C., Laverne, C., Godard, M., 2000. Petrography, Geochemistry and Physical Properties of a Continuous Extrusive Section from the Sarami Massif, Semail Ophiolite. Marine Geophysical Researches 21, 387–407.
El-Rahman, Y.A., Polat, A., Dilek, Y., Fryer, B.J., El-Sharkawy, M., Sakran, S., 2009. Geochemistry and tectonic evolution of the Neoproterozoic incipient arc-forearc crust in the Fawakhir area, Central Eastern Desert of Egypt. Precambrian Research 175, 116–134.
Elburg, M., Foden, J., 1998. Temporal changes in arc magma geochemistry, northern Sulawesi, Indonesia. Earth and Planetary Science Letters 163, 381–398.
Escuder-Viruete, J., Díaz de Neira, A., Hernáiz Huerta, P.P., Monthel, J., García Senz, J., Joubert, M., Lopera, E., Ullrich, T., Friedman, R., Mortensen, J., Pérez-Estaún, A., 2006. Magmatic relationships and ages of Caribbean island-arc tholeiites, boninites and related felsic rocks, Dominican Republic. Lithos 90, 161–186. http://dx.doi.org/10.1016/j.lithos.2007.01.008.
Escuder-Viruete, J., Friedman, R., Castillo-Carrión, M., Jabites, J., Pérez-Estaún, A., 2011. Origin and significance of the ophiolitic high-P mélanges in the northern

Caribbean convergent margin: insights from the geochemistry and large-scale structure of the Río San Juan metamorphic complex. Lithos 127, 483–504. http://dx.doi.org/10.1016/j.lithos.2011.09.015.
Ewart, A., Hergt, J.M., Hawkins, J.W., 1994. Major element, trace element, and isotope (Pb, Sr, and Nd) geochemistry of Site 839 Basalts and Basaltic Andesites: implications for arc volcanism. In: Hawkins, J., Parson, L., Allan, J., et al. (Eds.), Proceedings of the Ocean Drilling Program, Scientific Results, College Station, TX, Ocean Drilling Program, vol. 133, pp. 519–531.
Farahat, E.S., 2010. Neoproterozoic arc–back-arc system in the Central Eastern Desert of Egypt: evidence from supra-subduction zone ophiolites. Lithos 120, 293–308. http://dx.doi.org/10.1016/j.lithos.2010.08.017.
Feeley, T., Davidson, J., 1994. Petrology of calc-alkaline lavas at Volcan-Oollague and the origin of compositional diversità at central Andean stratovolcanoes. Journal of Petrology 35, 1295–1340.
Floyd, P.A., Kelling, G., Gökçen, S.L., Gökçen, N., 1991. Geochemistry and tectonic environment of basaltic rocks from the Misis Ophiolitic Melange, south Turkey. Chemical Geology 89, 263–280.
Floyd, P.A., Kryza, R., Crowley, Q.G., Winchester, J.A., Wahed, M.A., 2002. Sleza Ophiolite: geochemical features and relationship to Lower Palaeozoic rift magmatism in the Bohemian Massif. In: Winchester, J.A., Pharaoh, T.C., Verniers, J. (Eds.), Palaeozoic Amalgamation of Central Europe, Special Publications, vol. 201. Geological Society, London, pp. 197–215.
Francis, D., 2003. Cratonic mantle roots, remnants of a more chondritic Archean mantle? Lithos 71, 135–152. http://dx.doi.org/10.1016/S0024-4937(03)00110-5.
Gardien, V., Lécuyer, C., Moyen, J.-F., 2008. Dolerites of the Woodlark Basin (Papuan Peninsula, New Guinea): A geochemical record of the influence of a neighbouring subduction zone. Journal of Asian Earth Sciences 33, 139–154. http://dx.doi.org/10.1016/j.jseaes.2007.12.003.
Ghazi, A.M., Hassanipak, A.A., Mahoney, J.J., Duncan, R.A., 2004. Geochemical characteristics, 40Ar–39Ar ages and original tectonic setting of the Band-e-Zeyarat/Dar Anar ophiolite, Makran accretionary prism, S.E. Iran. Tectonophysics 393, 175–196. http://dx.doi.org/10.1016/j.tecto.2011.10.001.
Giunta, G., Beccaluva, L., Coltorti, M., Siena, F., Vaccaro, C., 2002. The southern margin of the Caribbean Plate in Venezuela: tectono-magmatic setting of the ophiolitic units and kinematic evolution. Lithos 63, 19–40.
Godard, M., Bosch, D., Einaudi, F., 2006. A MORB source for low-Ti magmatism in the Semail ophiolite. Chemical Geology 234, 58–78. http://dx.doi.org/10.1016/j.chemgeo.2006.04.005.
Göncüoglu, M.C., Gürsu, S., Tekin, U.K., Köksal, S., 2008. New data on the evolution of the Neotethyan oceanic branches in Turkey: Late Jurassic ridge spreading in the Intra-Pontide branch. Ofioliti 33, 153–164.
Göncüoglu, M.C., Sayit, K., Tekin, U.K., 2010. Oceanization of the northern Neotethys: geochemical evidence from ophiolitic melange basalts within the Izmir–Ankara suture belt, NW Turkey. Lithos 116, 175–187. http://dx.doi.org/10.1016/j.lithos.2010.01.007.
Griffin, W.L., O'Reilly, S.Y., Abe, N., Aulbach, S., Davies, R.M., Pearson, N.J., Doyle, B.J., Kivi, K., 2003. The origin and evolution of Archean lithospheric mantle. Precambrian Research 127, 19–41. http://dx.doi.org/10.1016/S0301-9268(03)00180-3.
Guilmette, C., Hébert, R., Wang, C., Villeneuve, M., 2009. Geochemistry and geochronology of the metamorphic sole underlying the Xigaze Ophiolite, Yarlung Zangbo Suture Zone, South Tibet. Lithos 112, 149–162. http://dx.doi.org/10.1016/j.lithos.2009.05.027.
Guivel, C., Lagabrielle, Y., Bourgois, J., Martin, H., Arnaud, N., Fourcade, S., Cotten, J., Maury, R.C., 2003. Very shallow melting of oceanic crust during spreading ridge subduction: origin of near-trench Quaternary volcanism at the Chile Triple Junction. Journal of Geophysical Research 108 (B7), 2345,. http://dx.doi.org/10.1029/2002JB002119.
Guo, A.L., Zhang, G.W., Sun, Y.G., Zheng, J.K., Liu, Y., Wang, J.Q., 2007. Geochemistry and spatial distribution of OIB and MORB in A'nyemaqen ophiolite zone: evidence of Majixue-shan ancient ridge-centered hotspot. Science China, Series D: Earth Sciences 50, 197–208.
Haase, K.M., 2002. Geochemical constraints on magma sources and mixing processes in Easter Microplate MORB (SE Pacific): a case study of plume-ridge interaction. Chemical Geology 182, 335–355.
Haase, K.M., Devey, C.W., Mertz, D.F., Stoffers, P., Garbe-Schönberg, D., 1996. Geochemistry of lavas from Mohns Ridge, Norwegian-Greenland Sea: implications for melting conditions and magma sources near Jan Mayen. Contributions to Mineralogy and Petrology 123, 223–237.
Haase, K.M., Mühe, R., Stoffers, P., 2000. Magmatism during extension of the lithosphere: geochemical constraints from lavas of the Shaban Deep, northern Red Sea. Chemical Geology 166, 225–239. http://dx.doi.org/10.1016/S0009-2541(99)00221-1.
Haase, K.M., Devey, C.W., Wieneke, M., 2003. Magmatic processes and mantle heterogeneity beneath the slow-spreading northern Kolbeinsey Ridge segment, North Atlantic. Contributions to Mineralogy and Petrology 144, 428–448.
Harper, G.D., 2003. Tectonic implications of boninite, arc tholeiite, and MORB magma types in the Josephine Ophiolite, California-Oregon. In: Dilek, Y., Robinson, E.T. (Eds.), Ophiolites in Earth History, Special Publications, vol. 218. Geological Society of London, pp. 207–230.
Hastie, A.R., Kerr, A.C., Mitchell, S.F., Millar, I.L., 2008. Geochemistry and petrogenesis of Cretaceous oceanic plateau lavas in eastern Jamaica. Lithos 101, 323–343. http://dx.doi.org/10.1016/j.lithos.2007.08.003.
Hauff, F., Hoernle, K., Schmincke, H.-U., Werner, R., 1997. A Mid-Cretaceous origin for the Galapagos hotspot: volcanological, petrological and geochemical evidence from Costa Rican oceanic crustal fragments. Geologische Rundschau 86, 141–155.
Hauff, F., Hoernle, K., van der Bogaard, P., Alvarado, G., Garbe-Schonberg, D., 2000. Age and geochemistry of basaltic complexes in western Costa Rica: contributions to the geotectonic evolution of Central America. Geochemistry, Geophysics, Geosystems 1, 1009. http://dx.doi.org/10.1029/1999GC000020.
Hergt, J.M., Hawkesworth, C.J., 1994. Pb-, Sd-, and Nd-isotopic evolution of the Lau Basin: implication for mantle dynamics during backarc opening. In: Hawkins, J., Parson, L., Allan, J., et al. (Eds.), Proceedings of the Ocean Drilling Program, Scientific Results, College Station, TX, Ocean Drilling Program, vol. 135, pp. 505–517.
Hoeck, V., Koller, F., Meisel, T., Onuzi, K., Kneringer, E., 2002. The Jurassic South Albanian ophiolites: MOR- vs. SSZ-type ophiolites. Lithos 65, 143–164.
Hoeck, V., Ionescu, C., Balintoni, I., Koller, F., 2009. The Eastern Carpathians "ophiolites" (Romania): remnants of a Triassic ocean. Lithos 108, 151–171. http://dx.doi.org/10.1016/j.lithos.2008.08.001.
Ichiyama, Y., Ishiwatari, A., Koizumi, K., 2008. Petrogenesis of greenstones from the Mino-Tamba belt, SW Japan: evidence for an accreted Permian oceanic plateau. Lithos 100, 127–146. http://dx.doi.org/10.1016/j.lithos.2007.06.014.
Insergueix-Filippi, D., Dupeyrat, L., Dimo, A., Vergély, P., Bébien, J., 2000. Albanian ophiolites: II – model of subduction zone infancy at a Mid-ocean ridge. Ofioliti 25, 47–53.
Ionescu, C., Hoeck, V., Tomek, C., Koller, F., Balintoni, I., Lucian, B., 2009. New insights into the basement of the Transylvanian Depression (Romania). Lithos 108, 172–191. http://dx.doi.org/10.1016/j.lithos.2008.06.004.
Janney, P.E., Le Roex, A.P., Carlson, R.L., 2005. Hafnium isotope and trace element constraints on the nature of mantle heterogeneity beneath the Central Southwest Indian Ridge. Journal of Petrology 46, 2427–2464.
Jian, P., Liu, D., Kröner, A., Zhang, Q., Wang, Y., Sun, X., Zhang, W., 2009. Devonian to Permian plate tectonic cycle of the Paleo-Tethys Orogen in southwest China (II): insights from zircon ages of ophiolites, arc/back-arc assemblages and within-plate igneous rocks and generation of the Emeishan CFB province. Lithos 113, 767–784. http://dx.doi.org/10.1016/j.lithos.2009.04.004.
Jones, G., Robertson, A.H.F., 1991. Tectono-stratigraphic evolution of the Mesozoic Pindos ophiolite and related units, northwestern Greece. Journal of the Geological Society of London 148, 267–288.
Kamenetsky, V.S., Everard, J.L., Crawford, A.J., Varne, R., Eggins, S.M., Lanyon, R., 2000. Enriched end-member of primitive MORB melts: petrology and geochemistry of glasses from Macquarie Island (SW Pacific). Journal of Petrology 41, 411–430.
Karsten, J.L., Klein, E.M., Sherman, S.B., 1996. Subduction zone geochemical characteristics in ocean ridge basalts from the southern Chile Ridge: implications of modern ridge subduction systems for the Archean. Lithos 37, 143–161. http://dx.doi.org/10.1016/0024-4937(95)00034-8.
Kenney, B.C., 1982. Beware of spurious self-correlations! Water Resources Research 18, 1041–1048.
Kerr, A.C., Tarney, J., Marriner, G.F., Klaver, G.T., Saunders, A.D., Thirlwall, M.F., 1996. The geochemistry and petrogenesis of the late-Cretaceous picrites and basalts of Curacao, Netherlands Antilles: a remnant of an oceanic plateau. Contributions to Mineralogy and Petrology 124, 29–43.
Kerr, A.C., Tarney, J., Nivia, A., Marriner, G.F., Saunders, A.D., 1998. The internal structure of oceanic plateaus: inferences from obducted Cretaceous terranes in western Colombia and the Caribbean. Tectonophysics 292, 173–188.
Koglin, N., Kostopoulos, D., Reischmann, T., 2009a. Geochemistry, petrogenesis and tectonic setting of the Samothraki mafic suite, NE Greece: trace-element, isotopic and zircon age constraints. In: Robertson, A.H.F. (Ed.), Tethyan Tectonics of the Mediterranean Region: Some Recent Advances. Tectonophysics 473, pp. 53–68. http://dx.doi.org/10.1016/j.tecto.2008.10.028.
Koglin, N., Kostopoulos, D., Reischmann, T., 2009b. The Lesvos mafic-ultramafic complex, Greece: ophiolite or incipient rift? Lithos 108, 243–261. http://dx.doi.org/10.1016/j.lithos.2008.09.006.
Kronmal, R.A., 1993. Spurious correlation and the Fallacy of the ratio Standard revisited. Journal of the Royal Statistical Society: Series A (Statistics in Society) 156, 379–392.
Kuh, E., Meyer, J.R., 1955. Correlation and regression estimates when the data are ratios. Econometrica 23, 400–416.
Kumar, K.V., Ernst, W.G., Leelanandam, C., Wooden, J.L., Grove, M.J., 2010. First Paleoproterozoic ophiolite from Gondwana: geochronologic–geochemical documentation of ancient oceanic crust from Kandra, SE India. Tectonophysics 487, 22–32.
Lapierre, H., Dupuis, V., Lépinay, B.M., Bosch, D., Monié, P., Tardy, M., Maury, R.C., Hernandez, J., Polvé, M., Yeghicheyan, D., Cotten, J., 1999. Late Jurassic oceanic crust and upper cretaceous caribbean plateau Picritic basalts exposed in the Duarte igneous complex, Hispaniola. Journal of Geology 107, 193–207.
Lapierre, H., Samper, A., Bosch, D., Maury, R.C., Béchennec, F., Cotten, J., Demant, A., Brunet, P., Keller, F., Marcoux, J., 2004. The Tethyan plume: geochemical diversity of Middle Permian basalts from the Oman rifted margin. Lithos 74, 167–198.
Lassiter, J.C., Blichert-Toft, J., Hauri, E.H., Barsczus, H.G., 2004. Isotope and trace element variations in lavas from Raivavae and Rapa, Cook-Austral Islands: constraints on the nature of HIMUand EM-mantle and the origin of mid-plate volcanism in French Polynesia. Chemical Geology 202, 115–138.

Lewis, J.F., Viruete, J.E., Huerta, P.P.H., Gutierrez, G., Draper, G., Pérez-Estaun, A., 2002. Subdivisión geoquímica del Arco Isla Circum-Caribeño, Cordillera Central Dominicana: Implicaciones para la formación, acrecion y crecimiento cortical en un ambiente intraoceánico. Acta Geologica Hispanica 37, 81–122.

Li, X.-H., Zhao, J.-X., McCulloch, M.T., Zhou, G.-q., Xing, F.-m., 1997. Geochemical and Sm-Nd isotopic study of Neoprotcrozoic ophiolites from southeastern China; petrogenesis and tectonic implications. Precambrian Research 8, 129–144.

Lugovic, B., Altherr, R., Raczek, I., Hofmann, A.W., Majer, V., 1991. Geochemistry of peridotites and mafic igneous rocks from the Central Dinaric Ophiolite Belt, Yugoslavia. Contributions to Mineralogy and Petrology 106, 201–216.

Mahoney, J.J., Graham, D.W., Christie, D.G., Johnson, K.T.M., Hall, L.S., VonderHaar, D.L., 2002. Between a hot spot and a cold spot: isotopic variation in the Southeast Indian Ridge asthenosphere, 86°–118°E. Journal of Petrology 43, 1155–1176. http://dx.doi.org/10.1093/petrology/43.7.1155.

Maillet, P., Ruellan, E., Gérard, M., Person, A., Bellon, H., Cotten, J., Joron, J.-L., Nakada, S., Price, R.C., 1995. Tectonics, magmatism, and evolution of the New Ebrides Backarc Troughs (Southwest Pacific). In: Taylor, B. (Ed.), Backarc Basins, Tectonics and Magmatism. Plenum Press, New York, pp. 177–235.

Malinovsky, A.I., Golozoubov, V.V., Simanenko, V.P., Simanenko, L.F., 2008. Kema terrane: a fragment of a back-arc basin of the early Cretaceous Moneron-Samarga island-arc system, East Sikhote-Alin range, Russian Far East. Island Arc 17, 285–304.

Malpas, J., Zhou, M.-F., Robinson, P.T., Reynolds, P.H., 2003. Geochemical and geochronological constraints on the origin and emplacement of the Yarlung Zangbo ophiolites, Southern Tibet. Ophiolites in Earth History. In: Dilek, Y., Robinson, P.T. (Eds.), Ophiolites in Earth History, Geological Society of London Special Publications, vol. 218, pp. 191–206.

Mamberti, M., Lapierre, H., Bosch, D., Jaillard, E., Ethiene, R., Hernandez, J., Polvé, M., 2003. Accreted fragments of the Late Cretaceous Caribbean-Colombian Plateau in Ecuador. Lithos 66, 173–199.

Marroni, M., Pandolfi, L., Saccani, E., Zelic, M., 2004. Boninites from the Kopaonik area (southern Serbia): new evidences for suprasubduction ophiolites in the Vardar Zone. Ofioliti 29, 251–254.

Maury, R.C., Pubellier, M., Rangin, C., Wulput, L., Cotten, J., Soquet, A., Bellon, H., Guillaud, J.-P., Htun, H.M., 2004. Quaternary calc-alkaline and alkaline volcanism in an hyper-oblique convergence setting, central Myanmar and western Yunnan. Bulletin de la Societé géologique de France 175, 461–472.

Maxeiner, R.O., Corrigan, D., Harper, C.T., MacDougall, D.G., Ansdell, K., 2005. Paleoproterozoic arc and ophiolitic rocks on the northwest-margin of the Trans-Hudson Orogen, Saskatchewan, Canada: their contribution to a revised tectonic framework for the orogen. Precambrian Research 136, 67–106.

McKenzie, D., O'Nions, R.K., 1991. Partial melt distributions from inversion of rare Earth element concentrations. Journal of Petrology 32, 1021–1091.

Meschede, M., 1986. A method of discriminating between different types of mid-Ocean ridge basalts and continental tholeiites with the Nb-Zr-Y diagram. Chemical Geology 56, 207–218.

Metcalf, R.V., Wallin, E.T., Willse, K.R., Muller, E.R., 2000. Geology and geochemistry of the ophiolitic Trinity terrane, California: evidence of middle Paleozoic depleted supra-subduction zone magmatism in a proto-arc setting. In: Dilek, Y., Moores, E.M., Elthon, D., Nicolas, A. (Eds.), Ophiolites and Oceanic Crust: New Insights from Field Studies and the Ocean Drilling Program, Special Paper, vol. 349. Geological Society of America, pp. 403–418.

Metzger, E.P., Miller, R.B., Harper, G.D., 2002. Geochemistry and tectonic setting of the ophiolitic Ingalls complex, North Cascades, Washington: implications for Correlations of Jurassic Cordilleran Ophiolites. Journal of Geology 110, 543–560.

Miao, L., Fan, W., Liu, D., Zhang, F., Shi, Y., Guo, F., 2008. Geochronology and geochemistry of the Hegenshan ophiolitic complex: implications for late-stage tectonic evolution of the Inner Mongolia-Daxinganling Orogenic Belt, China. Journal of Asian Earth Sciences 32, 348–370.

Millward, D., Marriner, G.F., Saunders, A.D., 1984. Cretaceous tholeiitic volcanic rocks from the Western Cordillera of Colombia. Journal of the Geological Society of London 141, 847–860.

Mocek, B., 2001. Geochemical evidence for arc-type volcanism in the Aegean Sea: the blueschist unit of Siphnos, Cyclades (Greece). Lithos 57, 263–289.

Monjoie, P., Lapierre, H., Tashko, A., Mascle, G.H., Dechamp, A., Muceku, B., Brunet, P., 2008. Nature and origin of the Triassic volcanism in Albania and Othrys: a key to understanding the Neotethys opening? Bulletin de la Societé géologique de France 179, 411–425.

Monnier, C., Girardeau, J., Pubellier, M., Polvé, M., Permana, H., Bellon, H., 1999. Petrology and geochemistry of the Cyclops ophiolites (Irian Jaya, East Indonesia): consequences for the Cenozoic evolution of the north Australian margin. Mineralogy and Petrology 65, 1–28.

Monnier, C., Girardeau, J., Permana, H., Rehault, J.-P., Bellon, H., Cotten, J., 2003. Dynamics and age of formation of the Seram-Ambon ophiolites (Central Indonesia). Bulletin de la Societé géologique de France 174, 529–543.

Montanini, A., Tribuzio, R., Vernia, L., 2008. Petrogenesis of basalts and gabbros from an ancient continent–ocean transition (External Liguride ophiolites, Northern Italy). Lithos 101, 453–479. http://dx.doi.org/10.1016/j.lithos.2007.09.007.

Niu, Y., Collerson, K.D., Batiza, R., Wendt, J.I., Regelous, M., 1999. Origin of enriched-type mid-ocean ridge basalt at ridges far from mantle plumes: the East Pacific Rise at 11° 20′ N. Journal of Geophysical Research 104, 7067–7087.

Osozawa, S., Shinjo, R., Lo, C.-H., Jahn, B.-m., Hoang, N., Sasaki, M., Ishikawa, K., Kano, H., Hoshi, H., Xenophontos, C., Wakabayashi, J., 2012. Geochemistry and geochronology of the Troodos ophiolite: an SSZ ophiolite generated by subduction initiation and an extended episode of ridge subduction? Lithosphere 4, 497–510. http://dx.doi.org/10.1130/L205.1.

Pagé, P., Bédard, J.H., Tremblay, A., 2009. Geochemical variations in a depleted fore-arc mantle: the Ordovician Thetford Mines Ophiolite. Lithos 113, 21–47. http://dx.doi.org/10.1016/j.lithos.2009.03.030.

Parlak, O., Rızaoglu, T., Bagcı, U., Karaoglan, F., Höck, V., 2009. Tectonic significance of the geochemistry and petrology of ophiolites in southeast Anatolia, Turkey. In: Robertson, A.H.F., Parlak, O., Koller, F. (Eds.), Tethyan Tectonics of the Mediterranean Region: Some Recent Advances, Tectonophysics, vol. 473, pp. 173–187. http://dx.doi.org/10.1016/j.tecto.2008.08.002.

Pe-Piper, G., 1998. The nature of Triassic extension-related magmatism in Greece: evidence from Nd and Pb isotope geochemistry. Geological Magazine 135, 331–348.

Pearce, J.A., 1982. Trace element characteristics of lavas from destructive plate boundaries. In: Thorpe, R.S. (Ed.), Andesites. Wiley and Sons, New York, pp. 525–548.

Pearce, J.A., 2005. Mantle preconditioning by melt extraction during flow: theory and petrogenetic implications. Journal of Petrology 46, 973–997. http://dx.doi.org/10.1093/petrology/egi007.

Pearce, J.A., 2008. Geochemical fingerprinting of oceanic basalts with applications to ophiolite classification and the search for Archean oceanic crust. Lithos 100, 14–48. http://dx.doi.org/10.1016/j.lithos.2007.06.016.

Pearce, J.A., Cann, J.R., 1973. Tectonic setting of basic volcanic rock determined using trace elements analyses. Earth and Planetary Science Letters 19, 290–300.

Pearce, J.A., Norry, M.J., 1979. Petrogenetic implications of Ti, Zr, Y, and Nb variations in volcanic rocks. Contributions to Mineralogy and Petrology 69, 33–47.

Pearce, J.A., Stern, R.J., 2006. Origin of back-arc Basin magmas: trace element and isotope perspectives. In: Christie, D.M., Fisher, C.R., Lee, S.-M., Givens, S. (Eds.), Back-Arc Spreading Systems: Geological, Biological, Chemical, and Physical Interactions, Geophysical Monograph Series, vol. 166. American Geophysical Union, pp. 63–86.

Pearce, J.A., van der Laan, S.R., Arculus, R.J., Murton, B.J., Ishii, T., Peate, D.W., Parkinson, I.J., 1992. Boninite and harzburgite from Leg 125 (Bonin-Mariana forearc): a case study of magina genesis during the initial stage of subduction. In: Fryer, P., Pearce, J.A., Stokking, L.B., et al. (Eds.), Proceedings of the Ocean Drilling Program, Scientific Results, College Station, TX, Ocean Drilling Program, vol. 125, pp. 623–659. http://dx.doi.org/10.2973/odp.proc.sr.125.172.1992.

Pearson, K., 1897. On a form of spurious correlation which may arise when indices are used in the measurement of organs. Proceedings of the Royal Society of London 60, 489–502.

Phipps Morgan, J., Morgan, W.J., 1999. Two-stage melting and the geochemical evolution of the mantle: a recipe for mantle plumpudding. Earth and Planetary Science Letters 170, 215–239.

Photiades, A., Saccani, E., 2006. Geochemistry and Tectono-Magmatic significance of HP/LT metaophiolites of the Attic-Cycladic zone in the Lavrion area (Attica, Greece). Ofioliti 31, 85–98.

Photiades, A., Saccani, E., Tassinari, R., 2003. Petrogenesis and tectonic setting of volcanic rocks from the Subpelagonian ophiolitic mélange in the Agoriani area (Othrys, Greece). Ofioliti 28, 121–135.

Proenza, J.A., Diaz-Martinez, R., Iriondo, A., Marchesi, C., Melgarejo, J.C., Gervilla, F., Garrido, C.J., Rodriguez-Vega, A., Lozano-Santacruz, R., Blanco-Moreno, J.A., 2006. Primitive Cretaceous island-arc volcanic rocks in eastern Cuba: the Téneme Formation. Geologica Acta 4, 103–121.

Rampone, E., Romairone, A., Abouchami, W., Piccardo, G.B., Hofmann, A.W., 2005. Chronology, petrology, and isotope geochemistry of the Erro-Tobbio peridotites (Ligurian Alps, Italy): records of late Palaeozoic lithospheric extension. Journal of Petrology 46, 799–827. http://dx.doi.org/10.1093/petrology/egi001.

Reynaud, C., Jaillard, E., Lapierre, H., Mamberti, M., Mascle, G.H., 1999. Oceanic plateau and island arcs of southwestern Ecuador: their place in the geodynamic evolution of northwestern South America. Tectonophysics 307, 235–254.

Robertson, A.H.F., 2007. Overview of tectonic settings related to the rifting and opening of Mesozoic ocean basins in the Eastern Tethys: Oman, Himalayas and Eastern Mediterranean regions. In: Karner, G., Manatschal, G., Pinheiro, L. (Eds.), Imaging, Mapping and Modelling Continental Lithosphere Extension and Breakup, Geological Society of London Special Publication, vol. 282, pp. 325–389.

Rolland, Y., Galoyan, G., Bosch, D., Sosson, M., Corsini, M., Fornari, M., Vérati, C., 2009. Jurassic Back-arc and hot-spot related series in the Armenian ophiolites – implications for the obduction process. Lithos 112, 163–187. http://dx.doi.org/10.1016/j.lithos.2009.02.006.

Saccani, E., Photiades, A., 2004. Mid-ocean ridge and supra-subduction affinities in the Pindos Massif ophiolites (Greece): implications for magma genesis in a proto-forearc setting. Lithos 73, 229–253.

Saccani, E., Photiades, A., 2005. Petrogenesis and tectono-magmatic significance of volcanic and subvolcanic rocks in the Albanide-Hellenide ophiolitic mélanges. The Island Arc 14, 494–516.

Saccani, E., Padoa, E., Tassinari, R., 2000. Preliminary data on the Pineto gabbroic massif and Nebbio Basalts: progress toward the geochemical characterization of Alpine Corsica Ophiolites. Ofioliti 25, 75–85.

Saccani, E., Nicolae, I., Tassinari, R., 2001. Tectono-magmatic setting of the Jurassic ophiolites from the South Apuseni Mountains (Romania): petrological and geochemical evidence. Ofioliti 26, 9–22.

Saccani, E., Photiades, A., Padoa, E., 2003a. Geochemistry, petrogenesis and tectono-magmatic significance of volcanic and subvolcanic rocks from the Koziakas Mélange (Western Thessaly, Greece). Ofioliti 28, 43–57.
Saccani, E., Padoa, E., Photiades, A., 2003b. Triassic mid-ocean ridge basalts from the Argolis Peninsula (Greece): new constraints for the early oceanization phases of the Neo-Tethyan Pindos basin. Ophiolites in earth history. In: Dilek, Y., Robinson, P.T. (Eds.), Ophiolites in Earth History, Geological Society of London Special Publications, vol. 218, pp. 109–127.
Saccani, E., Principi, G., Garfagnoli, F., Menna, F., 2008a. Corsica ophiolites: geochemistry and petrogenesis of basaltic and metabasaltic rocks. Ofioliti 33, 187–207.
Saccani, E., Photiades, A., Santato, A., Zeda, O., 2008b. New evidence for supra-subduction zone ophiolites in the Vardar zone from the Vermion massif (northern Greece): implication for the tectono-magmatic evolution of the Vardar oceanic basin. Ofioliti 33, 65–85.
Saccani, E., Bortolotti, V., Marroni, M., Pandolfi, L., Photiades, A., Principi, G., 2008c. The Jurassic association of backarc basin ophiolites and calc-alkaline volcanics in the Guevgueli Complex (northern Greece): implication for the evolution of the Vardar Zone. Ofioliti 33, 209–227.
Saccani, E., Photiades, A., Beccaluva, L., 2008d. Petrogenesis and tectonic significance of Jurassic IAT magma-types in the Hellenide ophiolites as deduced from the Rhodiani ophiolites (Pelagonian zone, Greece). Lithos 104, 71–84. http://dx.doi.org/10.1016/j.lithos.2007.11.006.
Saccani, E., Delavari, M., Beccaluva, L., Amini, S.A., 2010. Petrological and geochemical constraints on the origin of the Nehbandan ophiolitic complex (eastern Iran): implication for the evolution of the Sistan Ocean. Lithos 117, 209–228. http://dx.doi.org/10.1016/j.lithos.2010.02.016.
Saccani, E., Beccaluva, L., Photiades, A., Zeda, O., 2011. Petrogenesis and tectono-magmatic significance of basalts and mantle peridotites from the Albanian–-Greek ophiolites and sub-ophiolitic mélanges. New constraints for the Triassic–Jurassic evolution of the Neo-Tethys in the Dinaride sector. Lithos 124, 227–242. http://dx.doi.org/10.1016/j.lithos.2010.10.009.
Saccani, E., Azimzadeh, Z., Dilek, Y., Jahangiri, A., 2013a. Geochronology and petrology of the early carboniferous misho mafic complex (NW Iran), and implications for the melt evolution of Paleo-Tethyan rifting in Western Cimmeria. Lithos 162–163, 264–278. http://dx.doi.org/10.1016/j.lithos.2013.01.008.
Saccani, E., Allahyari, K., Beccaluva, L., Bianchini, G., 2013b. Geochemistry and petrology of the Kermanshah ophiolites (Iran): Implication for the interaction between passive rifting, oceanic accretion, and plume-components in the Southern Neo-Tethys Ocean. Gondwana Research 24, 392–411. http://dx.doi.org/10.1016/j.gr.2012.10.009.
Salavati, M., 2008. Petrology, geochemistry and mineral chemistry of extrusive alkalic rocks of the Southern caspian sea ophiolite, Northern Alborz, Iran: evidence of alkaline magmatism in Southern Eurasia. Journal of Applied Science 8, 2202–2216.
Sarifakioglu, E., Özen, H., Winchester, J.A., 2009. Petrogenesis of the Refahiye Ophiolite and its Tectonic Significance for Neotethyan Ophiolites Along the.zmir-Ankara-Erzincan Suture Zone. Turkish Journal of Earth Sciences 18, 187–207. http://dx.doi.org/10.3906/yer-0702-4.
Sarifakioglu, E., Dilek, Y., Sevin, M., 2014. Jurassic-Paleogene intraoceanic magmatic evolution of the Ankara Mélange, north-central Anatolia, Turkey. Solid Earth 5, 77–108, 10, 5194/se-5-77-2014.
Scarrow, J.H., Pease, V., Fleutelot, C., Dushin, V., 2001. The late Neoproterozoic Enganepe ophiolite, Polar Urals, Russia: an extension of the Cadomian arc? Precambrian Research 110, 255–275.
Schilling, J.-G., 1973. The Icelandic mantle plume: geochemical study of the Reykjanes Ridge. Nature 242, 565–571.
Seifert, K., Brunotte, D., 1996. Geochemistry of weathered mid-ocean ridge basalt and diabase clasts from Hole 899B in the Iberia Abyssal Plain. In: Whitmarsh, R.B., Sawyer, D.S., Klaus, A., Masson, D.G. (Eds.), Proceedings of the Ocean Drilling Program, Scientific Results College Station, TX, Ocean Drilling Program, vol. 149, pp. 497–515. http://dx.doi.org/10.2973/odp.proc.sr.149.225.1996.
Shen, S., Feng, Q., Yang, W.W., Zhang, Z., Chong, P.C.I., 2010. Study on the geochemical characteristics of ocean-ridge and oceanic-island volcanic rocks in the Nan-Uttaradit zone, northern Thailand. Chinese Journal of Geochemistry 29, 175–181. http://dx.doi.org/10.1007/s11631-010-0175-x.
Shervais, J.W., 1982. Ti-V plots and the petrogenesis of modern ophiolitic lavas. Earth and Planetary Science Letters 59, 101–118.
Shervais, J.W., 2001. Birth, death, and resurrection: the life cycle of suprasubduction zone ophiolites. Geochemistry, Geophysics, Geosystems 2. http://dx.doi.org/10.1029/2000GC000080.
Shervais, J.W., Schuman, M.M.Z., Hanan, B.B., 2005. The Stonyford Volcanic Complex: a Forearc Seamount in the Northern California Coast ranges. Journal of Petrology 46, 2091–2128. http://dx.doi.org/10.1093/petrology/egi048.
Shi, R., Yang, J., Xu, Z., Qi, X., 2008. The Bangong Lake ophiolite (NW Tibet) and its bearing on the tectonic evolution of the Bangong–Nujiang suture zone. Journal of Asian Earth Sciences 32, 438–457. http://dx.doi.org/10.1016/j.jseaes.2007.11.011.
Singh, A.K., Singh, N.I., Devi, L.D., Singh, R.K.B., 2012. Geochemistry of Mid-Ocean Ridge Mafic intrusives from the Manipur Ophiolitic Complex, Indo-Myanmar Orogenic Belt, NE India. Journal of the Gological Society of India 80, 231–240.
Sivell, W.J., McCulloch, M.T., 2001. Geochemical and Nd-isotopic systematics of the Permo-Triassic Gympie Group, southeast Queensland. Australian Journal of Earth Sciences 48, 377–393.
Sun, S.-s., McDonough, W.F., 1989. Chemical and isotopic-systematics of oceanic basalts: implications for mantle composition and processes. In: Saunders, A.D., Norry, M.J. (Eds.), Magmatism in Ocean Basins, Geological Society of London Special Publication, vol. 42, pp. 313–345.
Takashima, R., Nishi, H., Yoshida, T., 2002. Geology, petrology and tectonic setting of the Late Jurassic ophiolite in Hokkaido, Japan. Journal of Asian Earth Sciences 21, 197–215.
Tankut, A., Dilek, Y., Onen, P., 1998. Petrology and geochemistry of the Neo-Tethyan volcanism as revealed in the Ankara melange, Turkey. Journal of Volcanology and Geothermal Research 85, 265–284.
Tashko, A., Mascle, G.H., Muceku, B., Lappierre, H., 2009. Nd, Pb isotope and trace element signatures of the Triassic volcanism in Albania. The relationship to the NeoTethys opening. AJNTS 2, 3–23.
Taylor, B., Martinez, F., 2003. Back-arc Basin Basalt systematics. Earth and Planetary Science Letters 210, 481–497.
Thirlwall, M.F., Gee, M.A.M., Taylor, R.N., Murton, B.J., 2004. Mantle components in Iceland and adjacent ridges investigated using double-spike Pb isotope ratios. Geochimica et Cosmochimica Acta 68, 361–386.
Thompson, G.M., Malpas, J., Smith, I.E.M., 1997. The geochemistry of tholeiitic and alkalic plutonic suites within the Northland ophiolite, northern New Zealand; magmatism in a back arc basin. Chemical Geology 142, 213–223.
Tormey, D., Frey, F., Lopez-Escobar, L., 1995. Geochemistry of the active Azufre-Planchon-Peteroa volcanic complex, Chile (35°15'S) – Evidente for multiple sources and processes in a cordilleran arc magmatic system. Journal of Petrology 36, 265–298. http://dx.doi.org/10.1093/petrology/36.2.265.
Trubelja, F., Marchig, V., Burgath, K.P., Vujovic, Z., 1995. Origin of the Jurassic Tethyan Ophiolites in Bosnia: a Geochemical approach to tectonic setting. Geologica Croatica 48, 49–66.
Trubelja, F., Burgath, K.P., Marchig, V., 2004. Triassic magmatism in the area of the Central Dinarides (Bosnia and Herzegovina): geochemical resolving of tectonic setting. Geologica Croatica 57, 159–170.
Tsukanov, N.V., Kramer, W., Skolotnev, S.G., Luchitskaya, M.V., Seifert, W., 2007. Ophiolites of the Eastern Peninsulas zone (Eastern Kamchatka): age, composition, and geodynamic diversity. Island Arc 16, 431–456.
Turner, S., Hawkesworth, C., Rogers, N., King, P., 1997. U–Th isotope disequilibria and ocean island basalt generation in the Azores. Chemical Geology 139, 145–164.
Ustaszewski, K., Schmid, S.M., Lugovic, B., Schuster, R., Schaltegger, U., Bernoulli, D., Hottinger, L., Kounov, A., Fügenschuh, B., Schefer, S., 2009. Late Cretaceous intra-oceanic magmatism in the internal Dinarides (northern Bosnia and Herzegovina): implications for the collision of the Adriatic and European plates. Lithos 108, 106–125. http://dx.doi.org/10.1016/j.lithos.2008.09.010.
Verma, S.P., Guevara, M., Agrawal, S., 2006. Discriminating four tectonic settings: five new geochemical diagrams for basic and ultrabasic volcanic rocks based on log-ratio transformation of major-element data. Journal of Earth System Science 115, 485–528.
Vermeesch, P., 2006. Tectonic discrimination diagrams revisited. Geochemistry Geophysics Geosystems 7. http://dx.doi.org/10.1029/2005GC001092.
Wang, P., Glover, L., 1992. A tectonic test for the most commonly used geochemical discriminant diagrams and patterns. Earth Science Review 33, 111–131.
Wang, Z., Sun, S., Hou, Q., Li, J., 2001. Effect of melt-rock interaction on geochemistry in the Kudi ophiolite (western Kunlun Mountains, northwestern China): implication for ophiolite origin. Earth and Planetary Science Letters 191, 33–48.
Wang, W.-L., Aitchison, J.C., Lo, C.-H., Zeng, Q.-G., 2008. Geochemistry and geochronology of the amphibolite blocks in ophiolitic mélanges along Bangong-Nujiang suture, central Tibet. Journal of Asian Earth Sciences 33, 122–138.
Weaver, B.L., Wood, D.A., Tarney, J., Joron, J.-L., 1987. Geochemistry of ocean island basalts from the South Atlantic: Bouvet, St. Helena, Gough and Tristan da Cunha. In: Fitton, J.G., Upton, B.G.J. (Eds.), Alkaline Igneous Rocks, Geological Society of London Special Publication, vol. 30, pp. 253–267.
Wolde, B., Asres, Z., Desta, Z., Gonzales, J.J., 1996. Neopreterozoic zirconium-depleted boninite and tholeiitic series rocks from Adola, southern Ethiopia. Precambrian Research 80, 261–279.
Wood, D.A., 1980. The application of a Th-Hf-Ta diagram to problems of tectono-magmatic classification and to establishing the nature of crustal contamination of basaltic lavas of the British Tertiary volcanic province. Earth and Planetary Science Letters 50, 11–30.
Woodhead, J.D., Johnson, R.W., 1993. Isotopic and trace-element profiles across the New Britain island arc, Papua New Guinea. Contributions to Mineralogy and Petrology 113, 479–491.
Workman, R.K., Hart, S.R., 2005. Major and trace element composition of the depleted MORB mantle (DMM). Earth and Planetary Science Letters 231, 53–72. http://dx.doi.org/10.1016/j.epsl.2004.12.005.
Xia, B., Chen, G.-W., Wang, R., Wang, Q., 2008. Seamount volcanism associated with the Xigaze ophiolite, Southern Tibet. Journal of Asian Earth Sciences 32, 396–405. http://dx.doi.org/10.1016/j.jseaes.2007.11.008.
Xiao, L., He, Q., Pirajno, F., Ni, P., Du, J., Wei, Q., 2008. Possible correlation between a mantle plume and the evolution of Paleo-Tethys Jinshajiang Ocean: evidence from a volcanic rifted margin in the Xiaru-Tuoding area, Yunnan, SW China. Lithos 100, 112–126. http://dx.doi.org/10.1016/j.lithos.2007.06.020.
Xu, J.-F., Zhang, B.-r., Han, Y.-w, 2008. Geochemistry of the Mian-Lue ophiolites in the Qinling Mountains, central China: constraints on the evolution of the Qinling orogenic belt and collision of the North and South China Cratons.

Journal of Asian Earth Sciences 32, 336–347. http://dx.doi.org/10.1016/j.jseaes.2007.11.004.

Xu, J.-F., Castillo, P.R., 2004. Geochemical and Nd–Pb isotopic characteristics of the Tethyan asthenosphere: implications for the origin of the Indian Ocean mantle domain. Tectonophysics 393, 9–27. http://dx.doi.org/10.1016/j.tecto.2004.07.028.

Xu, J.-F., Castillo, P.R., Chen, F.-R., Niu, H.-C., Yua, X.-Y., Zhen, Z.-P., 2003. Geochemistry of late Paleozoic mafic igneous rocks from the Kuerti area, Xinjiang, northwest China: implications for backarc mantle evolution. Chemical Geology 193, 137–154.

Yang, G., Li, Y., Santosh, M., Yang, B., Yan, J., Zhang, B., Tong, L., 2012. Geochronology and geochemistry of basaltic rocks from the Sartuohai ophiolitic mélange, NW China: implications for a Devonian mantle plume within the Junggar Ocean. Journal of Asian Earth Sciences 59, 141–155. http://dx.doi.org/10.1016/j.jseaes.2012.07.020.

Yellappa, T., Chetty, T.R.K., Tsunogae, T., Santosh, M., 2010. The Manamedu Complex: geochemical constraints on Neoproterozoic suprasubduction zone ophiolite formation within the Gondwana suture in southern India. Journal of Geodynamics 50, 268–285.

Yigitbas, E., Kerrich, R., Ylmaz, Y., Elmas, A., Xie, Q., 2004. Characteristics and geochemistry of Precambrian ophiolites and related volcanics from the Istanbul-Zonguldak Unit, Northwestern Anatolia, Turkey: following the missing chain of the Precambrian South European suture zone to the east. Precambrian Research 132, 179–206.

Yuan, C., Sun, M., Zhou, M.-F., Xiao, W., Zhou, H., 2005. Geochemistry and petrogenesis of the Yishak Volcanic Sequence, Kudi ophiolite, West Kunlun (NW China): implications for the magmatic evolution in a subduction zone environment. Contributions to Mineralogy and Petrology 150, 195–211. http://dx.doi.org/10.1007/s00410-005-0012-0.

Yumul- Jr., G.P., Zhou, M.-F., Wang, C.Y., Zhao, T.-P., Dimalanta, C.B., 2008. Geology and geochemistry of the Shuanggou ophiolite (Ailao Shan ophiolitic belt), Yunnan Province, SW China: evidence for a slow-spreading oceanic basin origin. Journal of Asian Earth Sciences 32, 385–395. http://dx.doi.org/10.1016/j.jseaes.2007.11.007.

Zhai, Q.-G., Jahn, B.-M., Zhang, R.-Y., Wang, J., Su, L., 2011. Triassic Subduction of the Paleo-Tethys in northern Tibet, China: evidence from the geochemical and isotopic characteristics of eclogites and blueschists of the Qiangtang Block. Journal of Asian Earth Sciences 42, 1356–1370. http://dx.doi.org/10.1016/j.jseaes.2011.07.023.

Zhang, Q., Wang, Y., Zhou, G.Q., Qian, Q., Robinson, P.T., 2003. Ophiolites in China: their distribution, ages and tectonic settings. Ophiolites in Earth history. In: Dilek, Y., Robinson, P.T. (Eds.), Ophiolites in Earth History, Geological Society of London Special Publication, vol. 218, pp. 541–566. http://dx.doi.org/10.1144/GSL.SP.2003.218.01.28.